CHAPTER 7:
STUDY ON DURABILITY PROPERTIES OF CONCRETE

7.1 GENERAL

The durability properties of the concrete mainly depend on its curing age among the other factors. Porosity and chloride ion penetration of concrete decreases with increase in the curing age [311]. It is due to a rise in the amount of C-S-H gel, which ties together the cement particles into a firm entity [312]. The addition of mineral admixtures improves the durability properties of concrete because of the finer size of their particles as compared to the cement particles. The space left after the process of hydration is filled by the finer particles leading to the densification of the microstructure. This densification also improves the Interfacial Transition Zone (ITZ) [313].

The concrete contains a large number of air voids. These air voids (when present up to a permissible limit) tend to enhance the durability properties of concrete (mostly in colder regions) against freeze and thaw. They help in reducing the internal stresses in the concrete, the stresses which may have generated due to an increase in the volume of water on freezing. These air voids provide empty spaces to compensate for this increase in the volume of water [314]. Rigid pavements, in colder regions, are subjected to severe freezing and thawing and must be protected from these conditions. Thus it can be said that air entrainment is an essential segment of concrete for rigid pavements exposed to freezing and thawing conditions [315]. When the maximum size of aggregate in concrete is 20 mm, the air content of 3.5% in concrete under mild exposure is recommended [316].

The durability of concrete mainly depends on the properties of its pore structure and the magnitude of microcracks present in the hardened cement paste and along the periphery of aggregates [317]. The interconnectivity between pores in the microstructure of concrete (also known as the porosity of concrete) causes ingress of liquid into the concrete. When liquid flows through interconnected pores in the concrete, the strength of concrete decreases [318]. The ability of the liquid to penetrate concrete through these interconnected pores is known as the permeability of concrete [319]. The concrete having lower permeability shows higher resistance to ingress of water, chlorides, sulphates and other deleterious materials in comparison with concrete having higher permeability [320], [321]. The permeability of concrete mainly depends on the composition of the materials, duration as well as type of curing and pre-conditioning before the test [322], [323]. As per Karasin and Dogruyol (2014) [324], permeability is the answer to all predicaments related to the durability of concrete. The water absorption by immersion (also known as saturated water absorption) and permeability of concrete are interlinked [319]. Therefore, in the current study, the permeability of concrete admixed with rice straw ash and microsilica was analysed in terms of saturated water absorption.

The permeability test of concrete measures the rate at which the water permeates through concrete under the pressure head [325]. However, the ingress of water into rigid pavement due to pressure head is rare [307]. Also, the techniques needed to study the microstructure of concrete (for justifying the results of permeability test) are unmanageable and do not represent the original field environment [317]. Therefore, in the current study, sorptivity test was done as it represents the actual field conditions and determines the rate of water absorption of rice straw ash and microsilica admixed concrete by capillary action [326]. Also, coefficient of water absorption of

concrete was found out as it helps in forecasting the service life and improving the performance of concrete [327].

The corrosion of steel reinforcements poses a severe threat to the structural integrity of the reinforced concrete structures. The main reason behind the corrosion of steel reinforcement is the penetration of the chloride ions into concrete as they are inclined towards debilitating the bond between concrete and steel [328]. The measurement of penetration of chloride ions into concrete can also be related to its durability properties. Different SCMs tend to reduce the penetration of chloride ions into concrete by causing a reduction in the permeability and pore size of concrete. In the present study, the chloride ion penetration was determined by ponding method.

The acids containing chlorides and sulphates pose a severe threat to the concrete structures, especially in the urban and industrial sector. The degradation rate of concrete exposed to acids depends on the concentration of acid, exposure time, the chemical resistance of concrete etc. [329]. The acid attack on hydrated cement paste can be divided into two stages. The first stage is the reaction of an acid with $Ca(OH)_2$. The second stage, a reaction between acid and C-S-H, does not start until all of the $Ca(OH)_2$ in the hydrated cement paste is consumed in the first stage [330]. The reaction between aggressive molecules of acids and aggregates takes place at the hydrated cement paste and aggregate interface [331]. The type of aggregate greatly influences the resistance of concrete to acid attack. It has been observed by various researchers that calcareous aggregates like dolomite or limestone are highly vulnerable to acid attack because of their high solubility in acids [152], [208], [297], [307], [330], [332], [333]. Therefore, in case of concrete with calcareous aggregates, the harmful effects of acid attack are distributed uniformly between the aggregates and paste phases because of which

continuous neutralisation of acid takes place (by the aggregates from an exposed surface of concrete) [297]. For this reason, the calcareous aggregates are less prone to fall-out in a long term as they continue to neutralise the acids and are therefore preferred in construction of a concrete sewer [332], [334]. However, when siliceous aggregates like sandstone or granite are used in the concrete, only cement paste phase is damaged because siliceous aggregates are mostly immune to the acid attack [152], [208], [297], [307], [330], [332], [333]. For this reason, the siliceous aggregates are more prone to fall-out because of dissolution of the cement paste matrix around them [297].

Natural carbonation is the process of reaction of CO_2 present in the atmosphere with the hydration products of cement [192] while accelerated carbonation curing (ACC) is the artificial injection of CO_2 into a carbonation chamber at a predefined temperature and relative humidity. In the carbonation of both types, the main reaction product is calcium carbonate ($CaCO_3$). The formation of calcium carbonate increases the density of the concrete - subsequently, the permeability of concrete decreases [335]. Thus, when concrete is subjected to ACC for a shorter duration, positive effects of carbonation can be observed [336]. Also, both the carbonation processes decrease the pH value of concrete, and subsequently, concrete is bound to become less alkaline [153], [192], [337]. The pH of the pore solution of concrete falls from 12.5-13 to 8.3-9 during carbonation [179], [338]. Although ACC may positively affect the strength of concrete, it may also decrease the alkalinity of the concrete, causing corrosion in reinforcements. The water-cement (w/c) ratio also plays a vital role in ACC of concrete. It has been observed in the past that high w/c ratio leads to filling of pores in the concrete, which reduces the ingression of CO_2 into the concrete [339]. Also, the low w/c ratio hampers the reaction of CO_2 with C_3S and C_2S (in the case of ACC) [192]. The

range of favourable water-cement ratio (w/c) for ACC of cement paste and mortar was found to be between 0.05 and 0.13, and optimum w/c ratio was 0.125 [192], [340], [341]. However, concrete preparation is not possible at such low w/c ratios. As per the study by Shi and Wu (2008) [339], the optimum w/c ratio in concrete subjected to carbonation lies in the range of 0.36 to 0.43.

7.2 AIR ENTRAINMENT IN FRESH CONCRETE

The air content in fresh concrete of every mix is shown in Table 7.1. The air content in fresh concrete was constant when OPC was partially replaced by 15% or more RSA and MS. The least air content (3.6%) was found in the concrete of mix R10M7.5. In the past, researchers concluded that the HRWR does not significantly affect the air content in the fresh concrete [342]. They also found that the effect of water to total binder ratio (w/b) on the air content of fresh concrete is higher than the effect of amount and type of mineral admixtures. As the w/b ratio was constant in this study, it can be perceived that the decline in the air content was because of incorporation of RSA and MS. Based on the literature, this decline could be attributed to the filler as well as pozzolanic effect of rice straw ash and microsilica particles.

Table 7.1 Air content in fresh concrete

Mix	R0	R10	M2.5	M5	M7.5	M10	R5M5	R5M7.5	R10M5	R10M7.5
Air Content (%)	4.05	3.8	3.9	3.8	3.75	3.7	3.75	3.65	3.6	3.6

7.3 SATURATED WATER ABSORPTION

The saturated water absorption (SWA) of PQC admixed with rice straw ash and microsilica is given in Table 7.2 and shown in Figure 7.1. The percentage reduction in the saturated water absorption of concrete due to the admixing of RSA and MS is given in Table 7.3.

It is evident from the results that the saturated water absorption of concrete reduces with increase in the curing age. It could be attributed to a decrease in volume of permeable voids, as similar results were obtained in another study as well [135]. The saturated water absorption of concrete reduced due to admixing of rice straw ash and microsilica. The maximum percentage reduction of saturated water absorption in mix R10, M2.5, M5 and M7.5 w.r.t. R0 was obtained at 3 days of curing (15.50%, 10.79%, 12.83%, and 20.64% respectively) while the maximum percentage reduction of saturated water absorption in mix M10, R5M5, R5M7.5, R10M5, and R10M7.5 w.r.t R0 was obtained at 365 days of curing (36.45%, 28.57%, 31.20%, 38.55%, and 40.65% respectively). The minimum saturated water absorption was by mix R10M7.5 amongst all the tested mixes of concrete. As particles of microsilica and rice straw ash were finer than the OPC particles; it led to the reorientation of the structure of concrete, thus resulting in the dense packing. Also, the admixing of RSA and MS optimized the microstructure of the interfacial transition zone (ITZ). Comparable discoveries were also reported for concrete admixed with fly ash and sugarcane bagasse ash [21]. The densely packed concrete and optimized ITZ due to admixing of RSA and MS were visible in the SEM and petrographic analysis of the admixed concrete samples. MS was more effective in reducing the saturated water absorption of admixed concrete as compared to RSA due to its higher fineness and pozzolanicity. The saturated water absorption in mix R10 (10% RSA) at 28 days of curing was 3.31% while the saturated water absorption in mix M10 (10% MS) at 28 days of curing was 2.52%. A similar pattern was observed at other days of curing also.

Table 7.2 Saturated water absorption (%)

Curing Age (days)	Mix									
	R0	**R10**	**M2.5**	**M5**	**M7.5**	**M10**	**R5M5**	**R5M7.5**	**R10M5**	**R10M7.5**
3	4.3	3.63	3.83	3.75	3.41	2.93	3.41	3.24	2.89	2.79
7	3.83	3.41	3.61	3.53	3.32	2.84	3.18	3.14	2.83	2.62
28	3.53	3.31	3.4	3.35	3.15	2.52	2.68	2.52	2.33	2.26
60	2.94	2.76	2.82	2.82	2.64	2.06	2.20	2.12	1.94	1.86
90	2.82	2.59	2.65	2.64	2.54	1.87	2.00	1.98	1.76	1.69
365	2.38	2.25	2.33	2.3	2.19	1.51	1.7	1.64	1.46	1.41

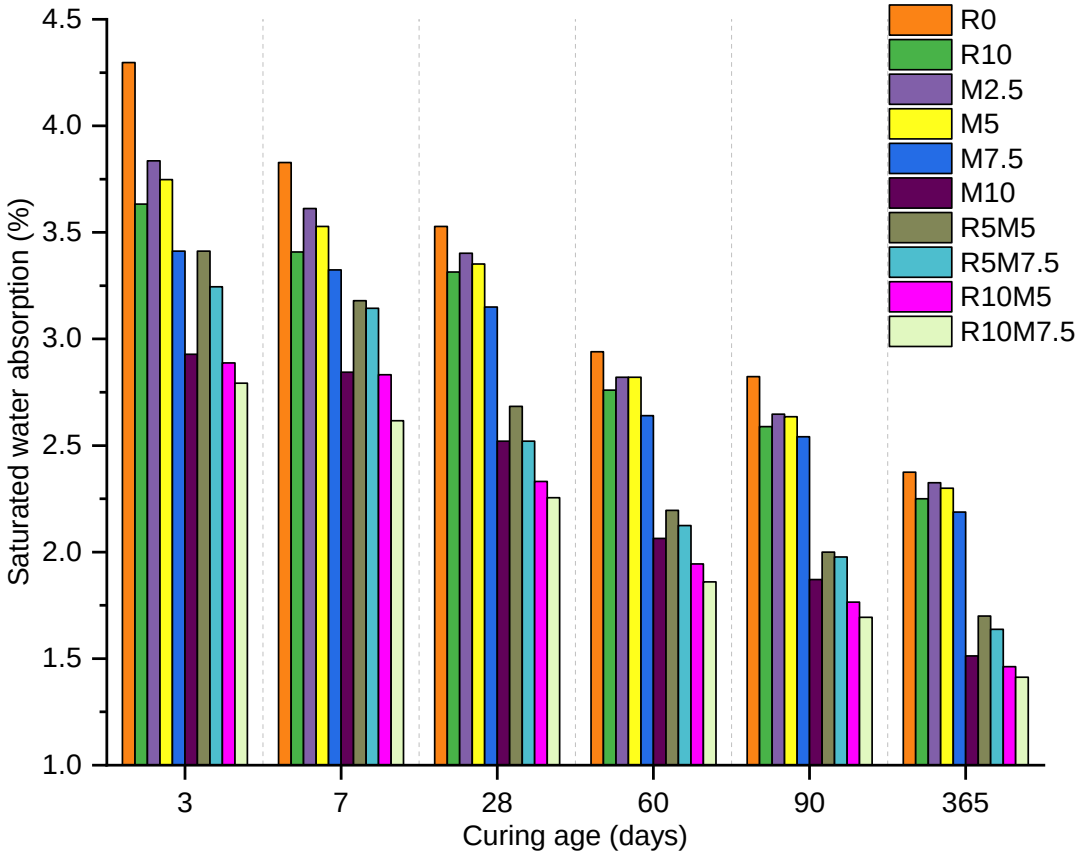

Figure 7.1 Saturated water absorption of various mix of concrete

Table 7.3 Percentage reduction of SWA in admixed concrete w.r.t. R0

Curing Age (days)	Mix								
	R10	**M2.5**	**M5**	**M7.5**	**M10**	**R5M5**	**R5M7.5**	**R10M5**	**R10M7.5**
3	15.50	10.79	12.83	20.64	31.90	20.64	24.55	32.85	35.05
7	11.02	5.69	7.89	13.21	25.74	16.97	17.91	26.06	31.70
28	6.12	3.63	5.05	10.76	28.61	23.97	28.61	33.97	36.11
60	6.12	4.08	4.08	10.20	29.80	25.31	27.76	33.88	36.73
90	8.22	6.13	6.55	9.89	33.67	29.08	29.91	37.42	39.92
365	5.46	2.31	3.36	8.09	36.45	28.57	31.20	38.55	40.65

7.4 RATE OF WATER ABSORPTION

The rate of water absorption (RoWA) or sorptivity of concrete admixed with rice straw ash and microsilica is given in Table 7.4 (initial rate of water absorption) and Table 7.5 (secondary rate of water absorption). The graph between curing age (days) and rate of water absorption is shown in Figure 7.2 (initial rate of water absorption) and Figure 7.3 (secondary rate of water absorption). Also, the percentage reduction in the RoWA of concrete due to admixing of RSA and MS is given in Table 7.6 (initial RoWA) and Table 7.7 (secondary RoWA).

Table 7.4 Initial rate of water absorption (x 10^{-6}m/$s^{0.5}$)

Curing Age (days)	Mix									
	R0	**R10**	**M2.5**	**M5**	**M7.5**	**M10**	**R5M5**	**R5M7.5**	**R10M5**	**R10M7.5**
3	12.38	9.51	11.48	11.38	8.11	6.98	8.04	7.1	5.36	5.17
7	10.14	9.01	9.79	9.7	8.01	5.75	7.63	6.47	5.3	4.98
28	5.9	5.36	5.62	5.49	5.27	5.22	5.24	5.22	5.19	4.09
60	5.55	5.15	5.29	5.21	4.85	4.73	4.76	4.75	4.67	3.48
90	5.14	4.65	5.13	4.9	4.63	4.29	4.48	4.37	4.05	3.37
365	5.04	4.42	4.97	4.7	4.35	3.9	4.17	4.13	3.61	3.03

Table 7.5 Secondary rate of water absorption (x 10^{-6}m/$s^{0.5}$)

Curing Age (days)	Mix									
	R0	**R10**	**M2.5**	**M5**	**M7.5**	**M10**	**R5M5**	**R5M7.5**	**R10M5**	**R10M7.5**
3	1.21	0.76	1.15	0.91	0.62	0.45	0.59	0.56	0.42	0.42
7	0.99	0.75	0.94	0.88	0.56	0.42	0.44	0.43	0.40	0.38
28	0.60	0.51	0.55	0.53	0.47	0.40	0.43	0.42	0.39	0.37
60	0.57	0.49	0.52	0.50	0.43	0.38	0.39	0.38	0.35	0.32
90	0.51	0.43	0.50	0.47	0.43	0.35	0.37	0.35	0.34	0.31
365	0.50	0.41	0.49	0.45	0.40	0.28	0.34	0.32	0.28	0.28

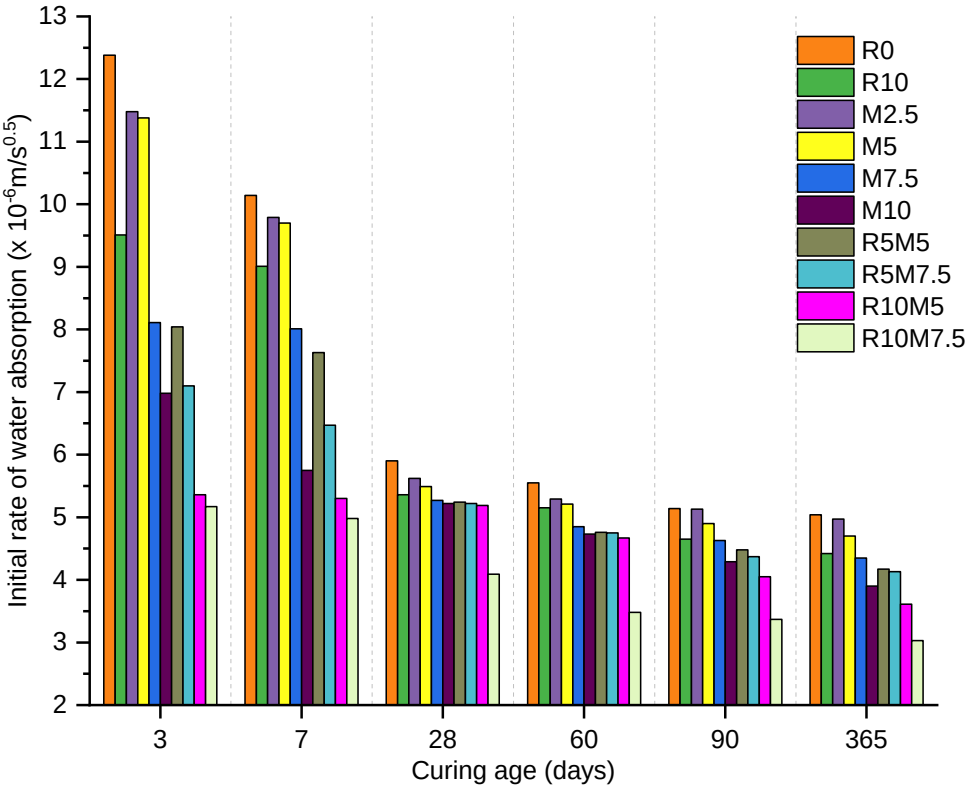

Figure 7.2 Initial rate of water absorption of various mix of concrete

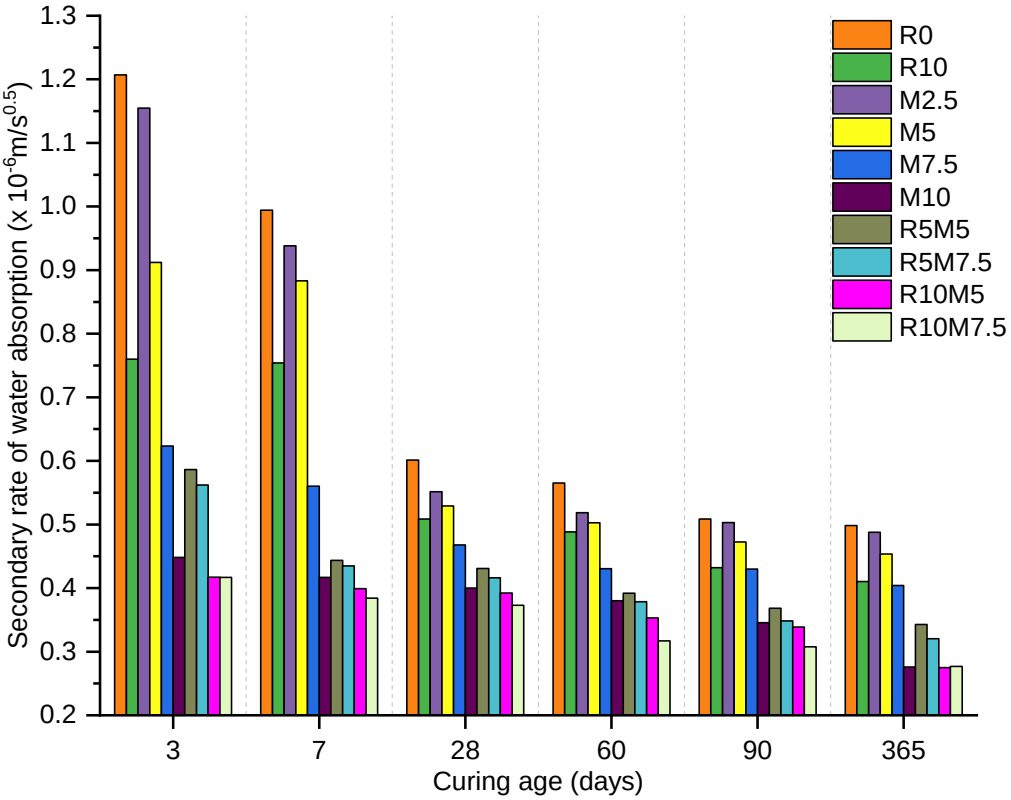

Figure 7.3 Secondary rate of water absorption of various mix of concrete

Table 7.6 Percentage reduction of initial RoWA in admixed concrete w.r.t. R0

Curing Age (days)	Mix								
	R10	**M2.5**	**M5**	**M7.5**	**M10**	**R5M5**	**R5M7.5**	**R10M5**	**R10M7.5**
3	23.18	7.27	8.08	34.49	43.62	35.06	42.65	56.70	58.24
7	11.14	3.45	4.34	21.01	43.29	24.75	36.19	47.73	50.89
28	9.15	4.75	6.95	10.68	11.53	11.19	11.53	12.03	30.68
60	7.21	4.68	6.13	12.61	14.77	14.23	14.41	15.86	37.30
90	9.53	0.19	4.67	9.92	16.54	12.84	14.98	21.21	34.44
365	12.30	1.39	6.75	13.69	22.62	17.26	18.06	28.37	39.88

Table 7.7 Percentage reduction of secondary RoWA in admixed concrete w.r.t. R0

Curing Age (days)	Mix								
	R10	**M2.5**	**M5**	**M7.5**	**M10**	**R5M5**	**R5M7.5**	**R10M5**	**R10M7.5**
3	37.03	4.34	24.43	48.36	62.86	51.41	53.43	65.44	65.47
7	24.16	5.64	11.17	43.66	58.08	55.38	56.27	59.87	61.37
28	15.41	8.26	11.98	22.19	33.44	28.36	30.78	34.77	37.96
60	13.61	8.26	11.05	23.85	32.74	30.65	32.99	37.55	43.90
90	15.08	1.12	7.09	15.51	32.09	27.56	31.50	33.39	39.54
365	17.68	2.13	8.99	18.96	44.68	31.26	35.70	44.82	44.47

The appreciable reduction in the initial rate of water absorption due to increase in the curing age was observed up to 7 days of curing of concrete. At later days of curing (28 days and beyond), the initial rate of water absorption of every concrete mix was approximately equal irrespective of the proportion of RSA and MS in the concrete except for mix R10M7.5 which showed significant reduction even at 365 days of curing. It was probably because the microstructure of concrete at 28 days of curing is much denser than at 7 days of curing due to formation of higher amount of C-S-H gel by hydration reaction which fills most of the empty voids. In all likelihood, this difference between the compactness of microstructure was further reduced when highly pozzolanic mineral admixtures like RSA and MS were used because at initial days of curing, the infilling of empty voids was also by additional C-S-H gel (produced by their pozzolanic action). The additional C-S-H gel was also produced during later stage of curing, but in a much smaller amount as compared to the initial stage due to high reactivity of RSA and MS. Therefore, for curing age beyond 28 days, the amount of water absorbed by admixed concrete by the process of capillary suction reduced

gradually. It implies that most of the voids were being infilled up to 28 days of curing (by additional C-S-H gel) and therefore the curing age beyond 28 days had an insignificant effect on the initial rate of water absorption of admixed concrete. It sits well with the results of strength test (compression/flexural/split tensile) in which most of the mixes of admixed concrete achieved 85-90% of 365 days strength at 28 days of curing itself. The initial rate of water absorption was minimum for concrete of mix R10M7.5 closely followed by mix R10M5.

Similar to the results of initial rate of water absorption, most of the reduction in secondary rate of water absorption in concrete due to admixing of RSA and MS was at 3 and 7 days of curing. However, when compared with the reduction in initial rate of water absorption at later days of curing, the reduction in secondary rate of water absorption of admixed concrete was comparatively noticeable. It implies that rice straw ash and microsilica were much more effective in reducing the secondary rate of water absorption as compared to the initial rate of water absorption. The secondary rate of water absorption was also minimum for concrete of mix R10M7.5 closely followed by mix R10M5.

Interfacial transition zone (ITZ) which surrounds the aggregates has a higher w/c ratio and fewer amounts of suspended cement particles as compared to the cement paste matrix. It results in higher porosity of the concrete. As the addition of MS and RSA had improved the cementitious paste system around the aggregates, it led to a reduction of w/b in ITZ. The addition of rice straw ash and microsilica reduced the preferred arrangement of C–S–H crystals [84]. That is why the rate of water absorption was lower for concrete admixed with microsilica and rice straw ash as compared to control concrete. In the past also, it has been observed that admixing of SCMs reduces

the rate of water absorption of concrete because of the densification of the cement paste [180], [343]. However, it also increases the chances of drying shrinkage because admixed concrete has little or no $Ca(OH)_2$ content as most of it takes part in the formation of additional C-S-H gel. In the absence of $Ca(OH)_2$, C-S-H gel collapses due to the removal of water from the pore system leading to drying shrinkage of the admixed concrete. Therefore, precautions should be taken while finalizing the proportion of mineral admixtures in the concrete.

7.5 COEFFICIENT OF WATER ABSORPTION

The coefficient of water absorption (CoWA) of admixed concrete at 3, 7, 28, 60, 90 and 365 days of curing is given in Table 7.8 and shown in Figure 7.4. Also, the percentage reduction in the CoWA of concrete due to admixing of RSA and MS is given in Table 7.9.

Table 7.8 Coefficient of water absorption (x 10^{-10} m^2/s)

Curing Age (days)	Mix									
	R0	**R10**	**M2.5**	**M5**	**M7.5**	**M10**	**R5M5**	**R5M7.5**	**R10M5**	**R10M7.5**
3	8.22	6.37	7.75	7.57	4	2.72	3.18	2.83	2.48	2.12
7	7.43	4	7.43	4.7	3.02	1.86	2.55	2.32	1.82	1.62
28	6.4	2.01	4.38	2.36	1.85	1.44	1.68	1.52	1.4	0.84
60	5.66	1.85	3.87	2.13	1.57	1.25	1.39	1.26	1.14	0.61
90	4.58	1.5	3.64	1.88	1.48	1.07	1.23	1.06	0.84	0.57
365	4.4	1.35	3.43	1.73	1.3	0.88	1.07	0.9	0.67	0.46

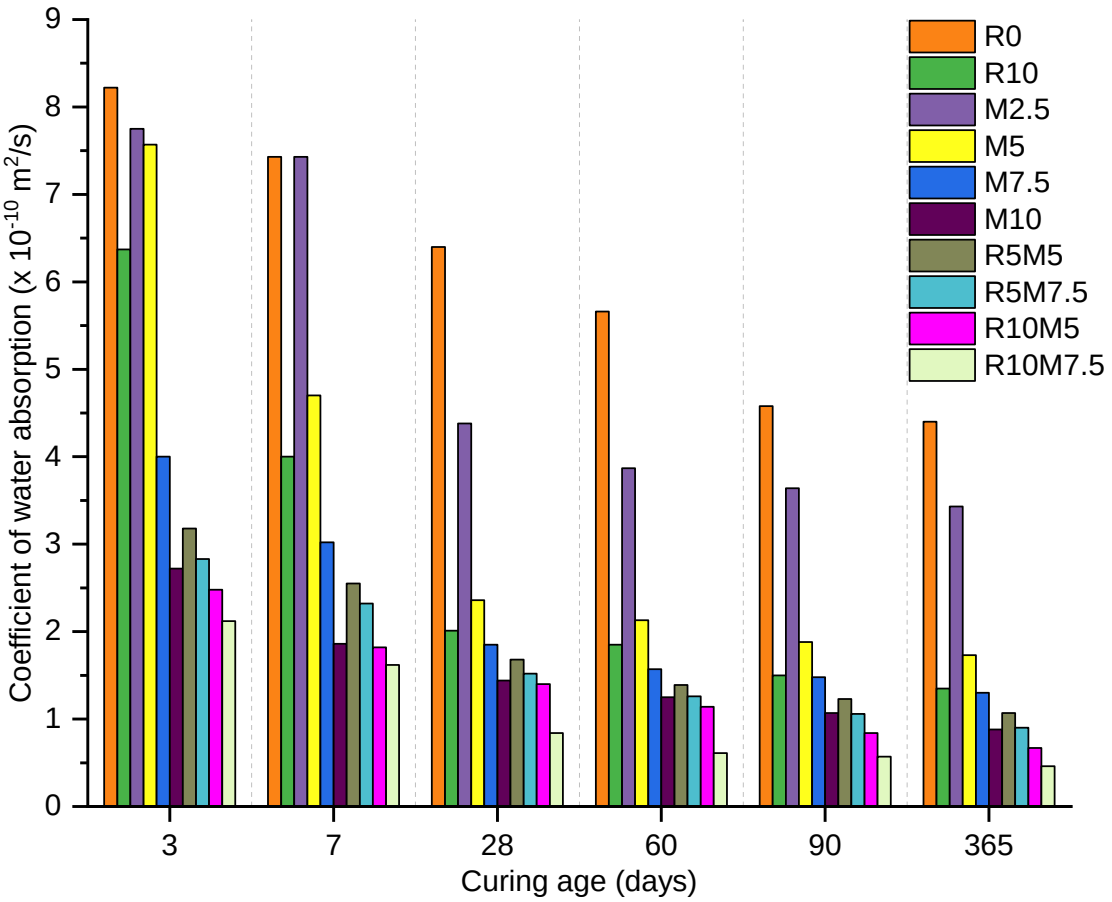

Figure 7.4 Coefficient of water absorption of various mix of concrete

Table 7.9 Percentage reduction of CoWA in admixed concrete w.r.t. R0

Curing Age (days)	Mix								
	R10	**M2.5**	**M5**	**M7.5**	**M10**	**R5M5**	**R5M7.5**	**R10M5**	**R10M7.5**
3	22.52	5.68	7.93	51.30	66.85	61.26	65.57	69.87	74.17
7	46.12	0.02	36.77	59.38	75.01	65.63	68.76	75.45	78.13
28	68.62	31.57	63.15	71.05	77.48	73.68	76.31	78.10	86.84
60	67.30	31.63	62.40	72.29	77.95	75.35	77.82	79.94	89.25
90	67.26	20.50	58.94	67.78	76.67	73.09	76.80	81.64	87.50
365	69.25	22.14	60.61	70.37	79.89	75.77	79.56	84.86	89.46

The results were similar to that of the rate of water absorption test and the saturated water absorption test. The effects of rice straw ash and microsilica on the coefficient of water absorption of concrete were more noticeable at initial days of curing. After that, at later days of curing, the coefficient of water absorption nearly becomes constant even with a higher proportion of RSA and MS in the mix. Thus it can be deduced that the later days of curing did not affect the coefficient of water

absorption of admixed concrete as much as the early days of curing did. The coefficient of water absorption was minimum for concrete mix R10M7.5. The percentage reduction in the coefficient of water absorption of mix R10M7.5 as compared to R0 was 74%, 78%, 87%, 89%, 87% and 89% at 3, 7, 28, 60, 90 and 365 days of curing respectively.

7.6 CHLORIDE ION PENETRATION

The penetration of chloride ions into concrete admixed with rice straw ash and microsilica is given in Table 7.10 (10-20 mm depth) and Table 7.11 (25-35 mm depth). The graph between curing age (days) and chloride ion penetration is shown in Figure 7.5 (10-20 mm depth) and Figure 7.6 (25-35 mm depth). Also, the percentage reduction in the penetration of chloride ions into concrete due to admixing of RSA and MS is given in Table 7.12 (10-20 mm depth) and Table 7.13 (25-35 mm depth).

Table 7.10 Chloride ions (%) at 10-20 mm depth

Curing Age (days)	Mix									
	R0	**R10**	**M2.5**	**M5**	**M7.5**	**M10**	**R5M5**	**R5M7.5**	**R10M5**	**R10M7.5**
3	1.41	1.20	1.30	1.24	1.16	0.98	1.13	1.02	0.95	0.89
7	1.35	1.16	1.28	1.23	1.12	0.76	0.86	0.79	0.65	0.53
28	0.71	0.64	0.68	0.67	0.58	0.42	0.46	0.44	0.42	0.41
60	0.69	0.56	0.66	0.58	0.54	0.42	0.44	0.43	0.39	0.36
90	0.69	0.54	0.65	0.56	0.51	0.40	0.43	0.42	0.24	0.23
365	0.68	0.54	0.65	0.56	0.49	0.26	0.43	0.40	0.18	0.14

Table 7.11 Chloride ions (%) at 25-35 mm depth

Curing Age (days)	Mix									
	R0	**R10**	**M2.5**	**M5**	**M7.5**	**M10**	**R5M5**	**R5M7.5**	**R10M5**	**R10M7.5**
3	1.36	1.20	1.26	1.24	1.13	0.95	1.06	0.99	0.92	0.80
7	1.31	1.12	1.24	1.19	1.02	0.74	0.82	0.76	0.55	0.48
28	0.69	0.64	0.67	0.65	0.55	0.42	0.44	0.42	0.41	0.37
60	0.66	0.54	0.58	0.57	0.54	0.39	0.43	0.42	0.39	0.33
90	0.65	0.53	0.58	0.55	0.51	0.38	0.42	0.41	0.24	0.20
365	0.65	0.50	0.57	0.55	0.49	0.24	0.40	0.28	0.18	0.13

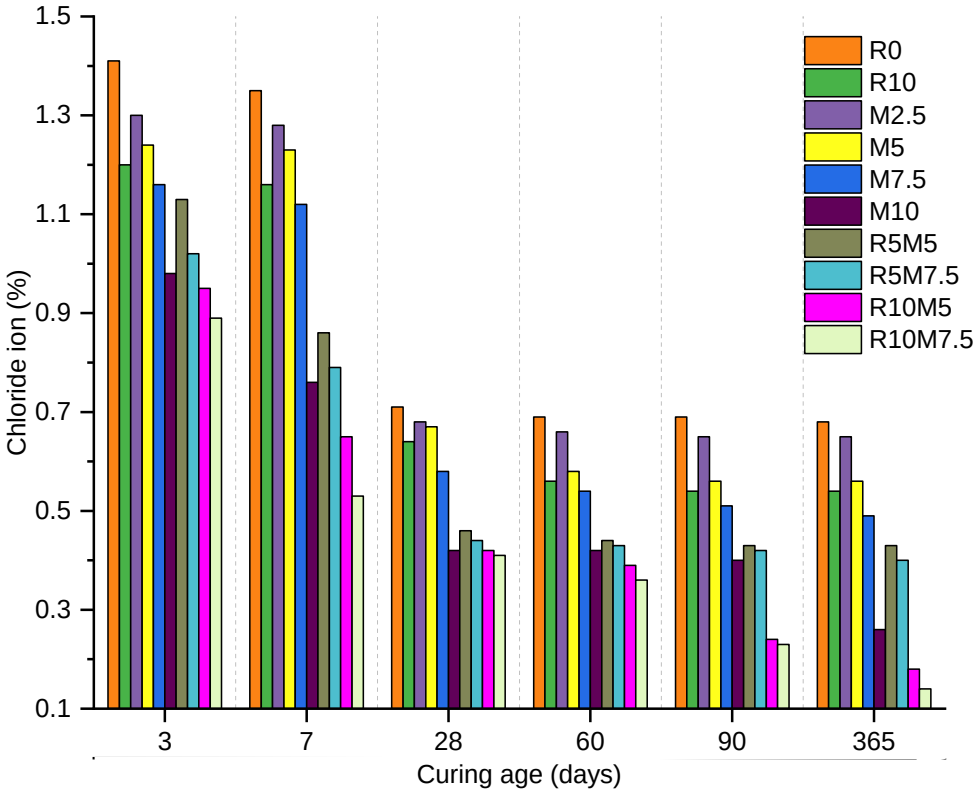

Figure 7.5 Percentage of chloride ions at 10-20 mm depth in concrete of different mix

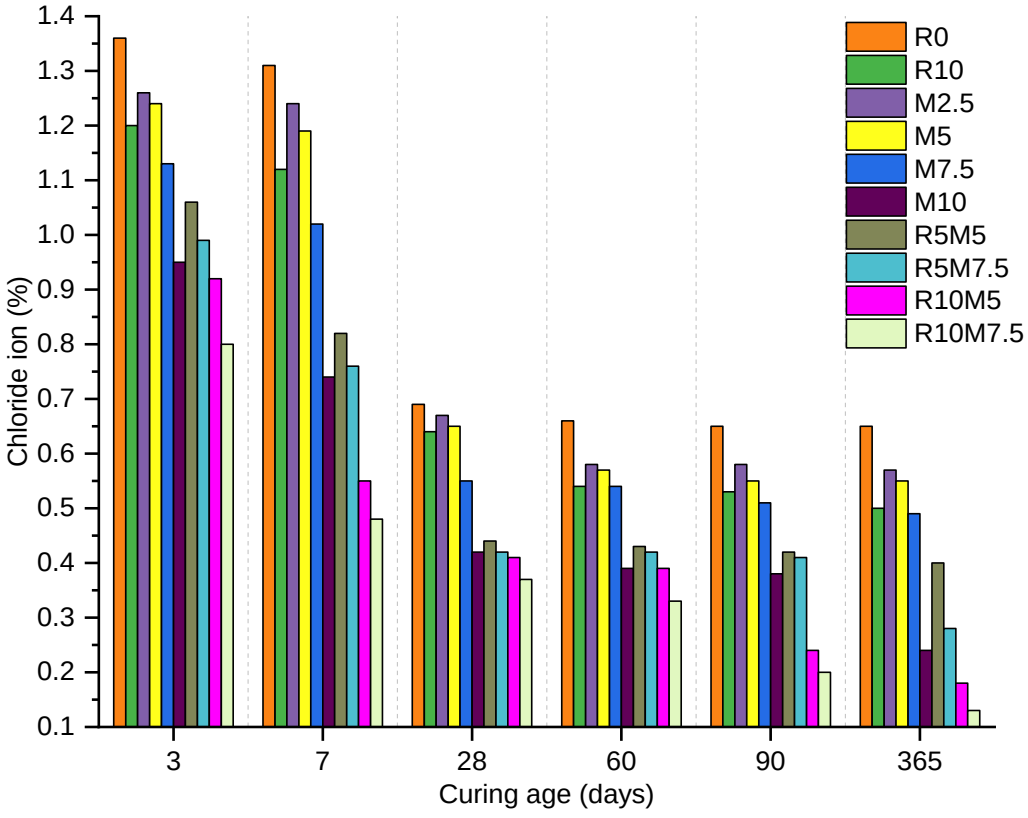

Figure 7.6 Percentage of chloride ions at 25-35 mm depth in concrete of different mix

Table 7.12 Percentage reduction of chloride ions in admixed concrete w.r.t. R0 (at 10-20 mm depth)

Curing Age (days)	Mix								
	R10	**M2.5**	**M5**	**M7.5**	**M10**	**R5M5**	**R5M7.5**	**R10M5**	**R10M7.5**
3	14.52	7.63	11.70	17.33	30.56	19.96	27.40	32.77	36.87
7	14.19	5.00	9.26	16.92	43.42	36.10	41.48	51.99	60.73
28	10.09	4.48	5.88	18.08	40.49	35.50	37.84	40.87	42.06
60	19.04	4.16	16.52	21.43	39.98	35.83	38.67	44.23	47.53
90	20.75	5.03	18.42	26.41	41.80	37.45	38.51	64.81	67.15
365	20.76	4.61	17.57	27.91	61.51	36.83	40.27	73.44	78.94

Table 7.13 Percentage reduction of chloride ions in admixed concrete w.r.t. R0 (at 25-35 mm depth)

Curing Age (days)	Mix								
	R10	**M2.5**	**M5**	**M7.5**	**M10**	**R5M5**	**R5M7.5**	**R10M5**	**R10M7.5**
3	11.71	7.63	8.81	17.33	30.02	21.79	27.42	32.65	39.38
7	14.19	5.00	9.26	21.91	43.42	37.26	41.48	58.10	62.29
28	7.60	3.27	5.88	20.76	39.22	35.84	38.57	39.79	45.81
60	18.01	12.41	14.04	19.09	40.63	35.69	36.93	41.84	47.65
90	19.15	11.34	16.06	22.51	41.59	34.89	37.14	63.25	66.93
365	22.89	11.44	15.32	24.43	63.42	37.36	57.13	72.31	75.08

There was reduction in the penetration of chloride ions into concrete with an increase in days of curing and was higher at a depth of 10-20 mm as compared to 25-35 mm depth. The reduction in the chloride ions at 10-20 mm depth with an increase in the curing age was significant up to 28 days of curing while at later days of curing (beyond 28 days), this rate of reduction was remarkably lower (similar to the results of water absorption test). For 10-20 mm depth, the percentage reduction in chloride ions when curing age was increased from 7 days to 28 days was 48%, 45%, 47%, 46%, 48%, 45%, 47%, 44%, 35% and 23% for concrete mix R0, R10, M2.5, M5, M7.5, M10, R5M5, R5M7.5, R10M5 and R10M7.5 respectively. Similarly, the percentage reduction in chloride ions when curing age was increased from 28 days to 60 days was 2%, 12%, 2%, 13%, 6%, 1%, 3%, 3%, 8% and 11% respectively. Therefore it can be said that the penetration of chloride ions at 10-20 mm depth of concrete was not affected by the curing age beyond 28 days and remained nearly constant. At 10-20 mm depth, the amount of chloride ion was lowest in the case of concrete mix R10M7.5. For 10-20 mm

depth, the percentage reduction in chloride ions in mix R10M7.5 w.r.t the control mix R0 was 36.87%, 60.73%, 42.06%, 47.53%, 67.15% and 78.94% at 3, 7, 28, 60, 90 and 365 days of curing respectively.

Similar to the results of penetration of chloride ions at 10-20 mm depth, most of the reduction in penetration of chloride ions (25-35 mm depth) was at 3, 7 and 28 days of curing. At 25-35 mm depth, the reduction in chloride ions with an increase in the curing age up to 28 days was higher than the reduction in chloride percentage at curing age beyond 28 days. For 25-35 mm depth, the percentage reduction in chloride ions when curing age was increased from 7 days to 28 days was 47%, 43%, 46%, 45%, 47%, 43%, 46%, 45%, 24% and 23% for concrete mix R0, R10, M2.5, M5, M7.5, M10, R5M5, R5M7.5, R10M5 and R10M7.5 respectively. Similarly, the percentage reduction in chloride ions when curing age was increased from 28 days to 60 days was 4%, 14%, 13%, 12%, 2%, 6%, 3%, 1%, 7% and 11% respectively. Similar to the observations of 10-20 mm depth, the chloride percentage at 25-35 mm depth was also not affected by the curing age beyond 28 days. At 25-35 mm depth, the amount of chloride ion was lowest in mix R10M7.5. For 25-35 mm depth, the percentage reduction in chloride ions in mix R10M7.5 w.r.t the control mix R0 was 39.38%, 62.29%, 45.81%, 47.65%, 66.93% and 75.08% at 3, 7, 28, 60, 90 and 365 days of curing respectively.

Both microsilica and rice straw ash improvised the resistance of concrete to penetration of chloride ions. It was mainly because particles of RSA and MS densifies the pore structure of concrete [311]. As microsilica and rice straw ash particles were finer than the OPC particles, they filled up the micro and macro pores of the concrete [100]. As per the literature, the higher resistance could also be due to the improved interfacial transition zone (ITZ) around the aggregates [344].

7.7 EFFECTS OF ACIDIC ENVIRONMENT

There is sufficient literature available which suggest that the deterioration of concrete under acidic environment can be assessed in terms of loss of mass and loss of compressive strength [332], [345]–[348]. Accordingly, concrete specimens in the present work were evaluated for an acid attack in terms of the loss of mass and loss of compressive strength. Ordinary Portland cement (OPC) is highly prone to acid attack since its hydration in the presence of water releases enormous amount of $Ca(OH)_2$. Subsequently, the reaction products of $Ca(OH)_2$ and acids reduce the alkalinity of cement paste [349]. However, OPC admixed with pozzolans is more acid-resistant [150], [190], [350]–[352]. The concrete admixed with pozzolans is influenced by the fineness of pozzolans and more specifically by the curing conditions [349], [353]. So, curing time of 28 days and 365 days were selected for the present work along with pozzolans (RSA and MS) finer than OPC.

7.7.1 Loss of Mass

The loss of mass due to immersion of concrete in acidic solutions is given in Table 7.14. The graph between different concrete mix and their loss of mass (%) is shown in Figure 7.7. Also, the percentage reduction in the loss of mass of concrete due to the admixing of RSA and MS is given in Table 7.15.

Table 7.14 Loss of mass (%) under 30 days immersion in acidic solution

Mix	28 days Water Curing		365 days Water Curing	
	HCl	H_2SO_4	HCl	H_2SO_4
R0	4.05	3.12	2.34	2.10
R10	3.47	2.88	2.01	1.74
M2.5	3.85	3.04	2.22	2.00
M5	3.66	2.96	2.11	1.80
M7.5	3.07	2.61	1.78	1.49
M10	2.37	2.16	1.37	1.23
R5M5	2.77	2.41	1.60	1.47
R5M7.5	2.54	2.26	1.47	1.25
R10M5	2.26	2.10	1.31	1.20
R10M7.5	2.19	2.09	1.27	1.14

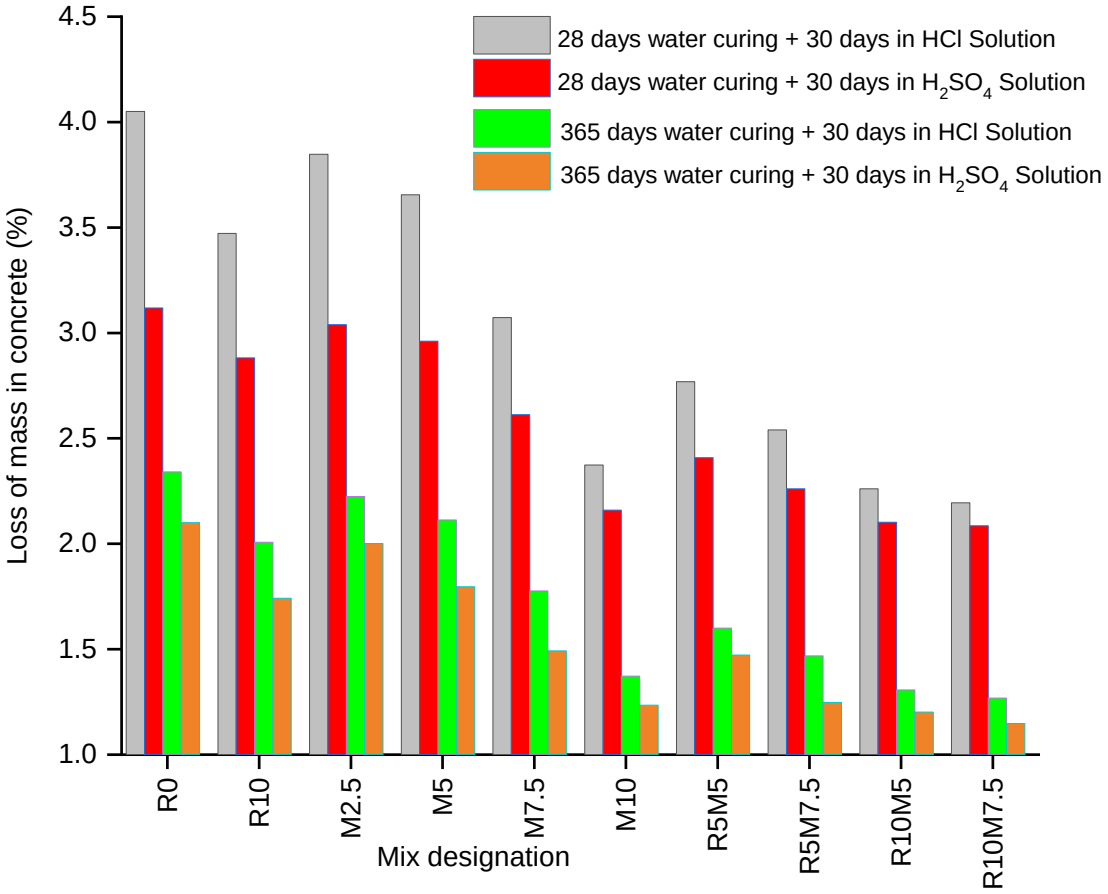

Figure 7.7 Percentage loss of mass in concrete

Table 7.15 Percentage reduction in loss of mass in admixed concrete w.r.t. R0

Mix	28 days Water Curing		365 days Water Curing	
	HCl	H_2SO_4	HCl	H_2SO_4
R10	14.26	7.63	14.22	17.05
M2.5	5.00	2.58	4.96	4.69
M5	9.75	5.11	9.71	14.48
M7.5	24.13	16.28	24.09	28.92
M10	41.39	30.77	41.37	41.20
R5M5	31.65	22.81	31.61	29.90
R5M7.5	37.29	27.55	37.26	40.58
R10M5	44.18	32.62	44.16	42.75
R10M7.5	45.81	33.17	45.78	45.63

The loss of mass was maximum in control mix R0 and minimum in mix R10M7.5. For 30 days of acidic immersion, concrete of every mix had a higher loss of mass at 28 days of curing in comparison with 365 days of water curing. For 30 days in HCl solution, the percentage loss of mass of R0 at 28 days and 365 days of curing was 4.05% and 2.34% respectively. At 28 days and 365 days of curing, the percentage loss of mass of R0 in H_2SO_4 solution was 3.12% and 2.10% respectively. For 30 days in HCl solution, the percentage loss of mass of other mixes (R10, M2.5, M5, M7.5, M10, R5M5, R5M7.5, R10M5 and R10M7.5) at 28 days of curing was 3.47, 3.85, 3.66, 3.07, 2.37, 2.77, 2.54, 2.26 and 2.19% respectively (Table 7.14). While for 30 days in H_2SO_4 solution, the percentage loss of mass of these mixes at 28 days of curing was 2.88, 3.04, 2.96, 2.61, 2.16, 2.41, 2.26, 2.1 and 2.09% respectively (Table 7.14). Clearly, damage to the concrete of each mix by hydrochloric acid was more significant as compared to damage by sulphuric acid. It was probably because of lower dissolvability of calcium sulphate (in case of H_2SO_4 immersion) in water in comparison with the dissolvability of calcium chloride (in case of HCl immersion).

The loss of mass of R10 (10% RSA) was more than the loss of mass of M10 (10% MS). Therefore it can be concluded that admixing of microsilica was more effective than admixing of rice straw ash in providing resistance to concrete in case of

acidic attack. RSA and MS particles fill in the gaps between the comparatively coarser cement particles in concrete which leads to higher packing density as compared to the control concrete R0. It led to a considerable reduction in the mass loss under acidic immersion. Due to better packing density and infilling of voids, the ability of the acids to penetrate into admixed concrete reduces considerably.

The difference between mass loss under two acidic solutions decreased with an increase in the amount of RSA and MS in concrete and was minimum for concrete of mix R10M7.5. At 28 days of curing, this difference in R0, R10, M2.5, M5, M7.5, M10, R5M5, R5M7.5, R10M5 and R10M7.5 was 0.93, 0.59, 0.81, 0.7, 0.46, 0.21, 0.36, 0.28, 0.16 and 0.1% respectively. Similarly, at 365 days of curing, this difference was 0.24, 0.27, 0.22, 0.32, 0.28, 0.14, 0.13, 0.22, 0.10 and 0.13% respectively. The above values indicate that the concrete on being subjected to a higher amount of curing hardens to an extent such that the ability of acidic solutions to ingress into concrete decreases drastically. Therefore, dissimilar effects of two different acidic solutions become similar with an increase in curing age of concrete.

7.7.2 Loss of Compressive Strength

The compressive strength of different concrete mix immersed in water for 28 and 365 days and then in acidic solutions for 30 days is given in Table 7.16 and shown in Figure 7.8 along with compressive strength at 58 and 395 days of water curing. The percentage loss of compressive strength of concrete when immersed in acidic solutions is given in Table 7.17 and shown in Figure 7.9.

Table 7.16 Compressive strength (MPa) of concrete mixes

Mix	Curing Condition					
	58 Days (Water)	28 Days (Water)		395 Days (Water)	365 Days (Water)	
		+ 30 Days (H_2SO_4)	+ 30 Days (HCl)		+ 30 Days (H_2SO_4)	+ 30 Days (HCl)
R0	51.57	48.46	47.74	53.12	51.42	49.57
R10	52.31	50.80	50.10	53.64	52.69	52.01
M2.5	54.76	53.12	52.10	56.72	55.56	54.85
M5	55.71	54.05	53.30	57.49	56.45	55.63
M7.5	56.41	54.78	54.10	57.75	56.76	56.16
M10	53.90	52.87	51.90	55.95	55.09	54.83
R5M5	53.20	52.05	51.20	55.31	54.45	54.05
R5M7.5	55.27	54.09	53.20	56.76	55.88	55.60
R10M5	52.87	51.89	50.95	54.16	53.35	53.24
R10M7.5	53.04	52.08	51.15	54.68	53.87	53.84

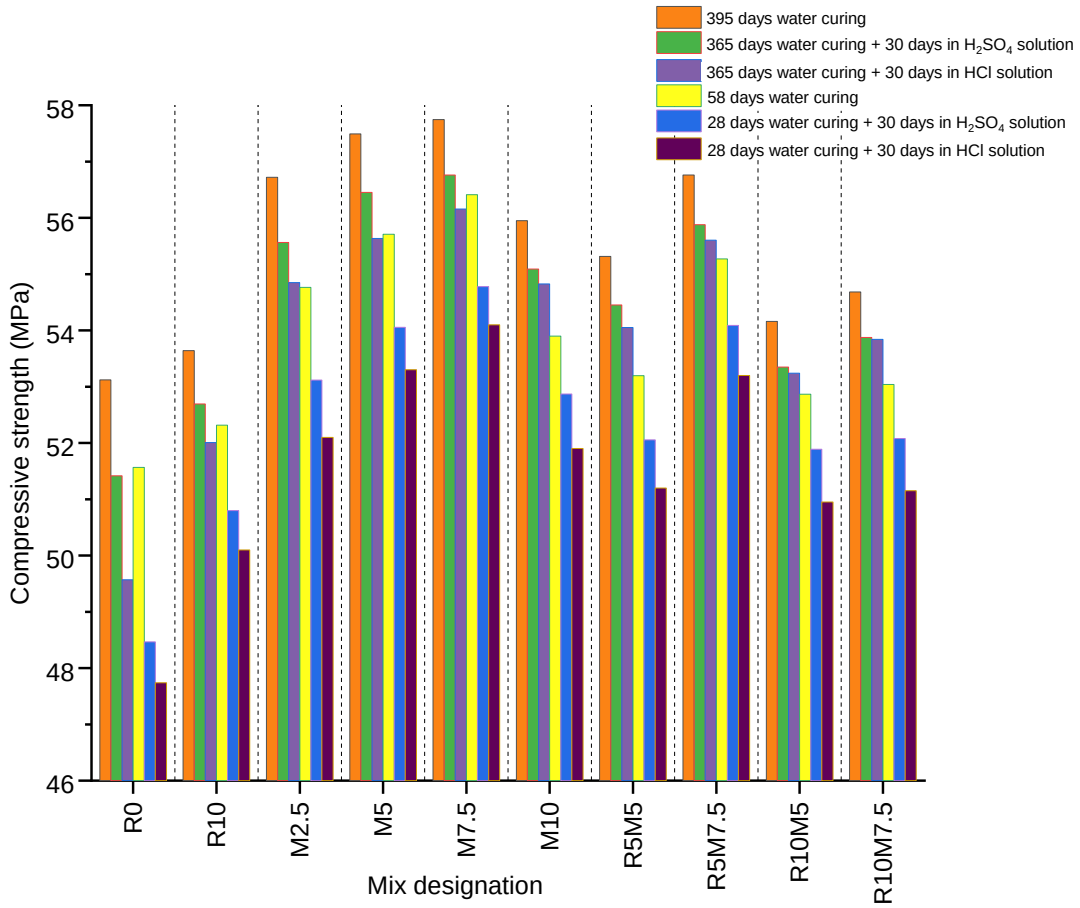

Table 7.8 Compressive strength of concrete mixes at different curing conditions

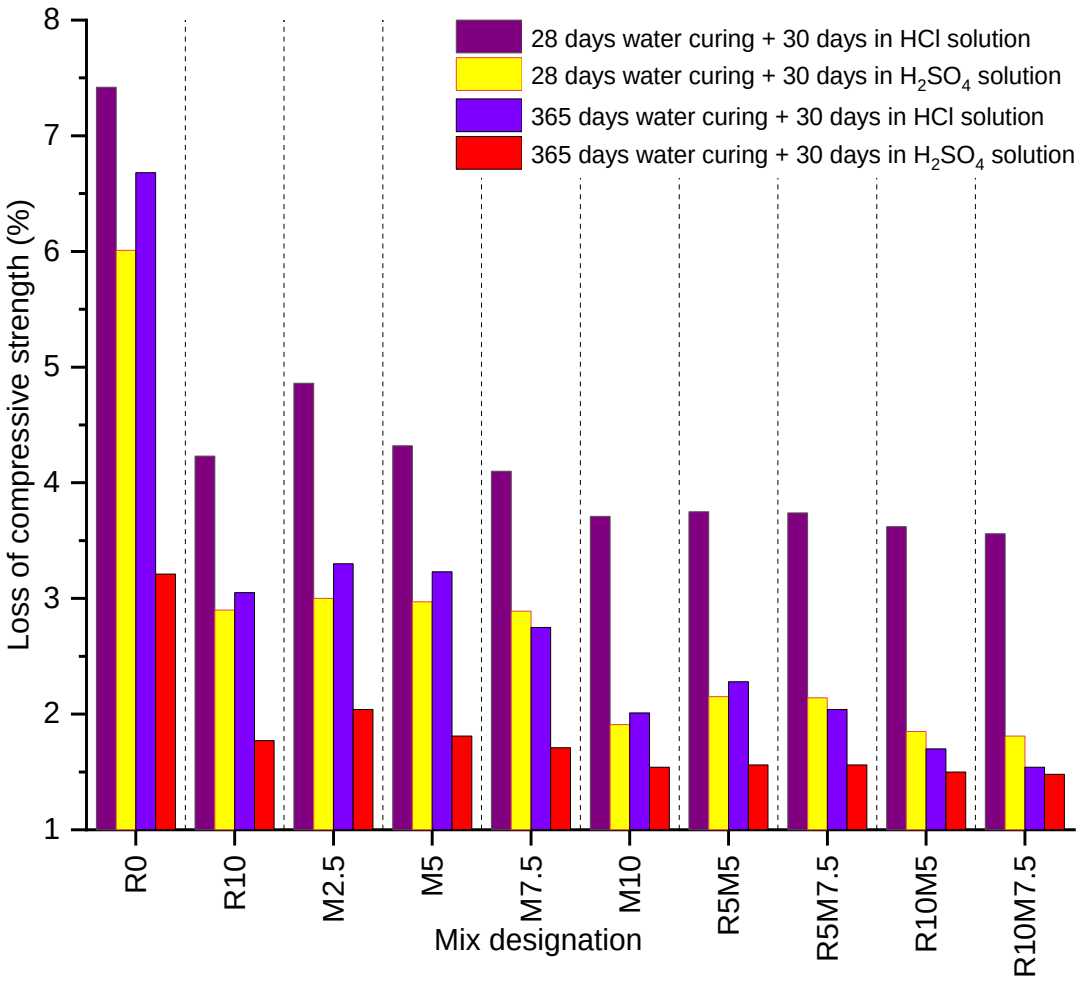

Table 7.9 Loss of compressive strength of concrete mixes at different curing conditions

Table 7.17 Loss of compressive strength (%)

Mix	Curing Condition			
	28 Days (Water)		365 Days (Water)	
	+ 30 Days (H_2SO_4)	+ 30 Days (HCl)	+ 30 Days (H_2SO_4)	+ 30 Days (HCl)
R0	6.01	7.42	3.21	6.68
R10	2.90	4.23	1.77	3.05
M2.5	3.00	4.86	2.04	3.30
M5	2.97	4.32	1.81	3.23
M7.5	2.89	4.10	1.71	2.75
M10	1.91	3.71	1.54	2.01
R5M5	2.15	3.75	1.56	2.28
R5M7.5	2.14	3.74	1.56	2.04
R10M5	1.85	3.62	1.50	1.70
R10M7.5	1.81	3.56	1.48	1.54

Higher compressive strengths were observed in concrete mixes subjected to water curing as compared to curing combination of water and acidic solution. The duration of water curing also had a profound impact on the resistance of concrete to acidic attack. The concrete admixed with RSA and MS were highly resistant to acid attack as they had comparatively low portlandite content (also found in XRD analysis and SEM analysis). The acids could have reacted with other hydration products in hardened cement paste however portlandite is more prone to attack by acids [354]. Similar outcomes were reported for other pozzolanic mineral admixtures also like fly ash, natural pozzolana etc. by other researchers [355], [356]. As MS had higher pozzolanicity and also because of its finer particle size, the resistance to an acidic solution was more in concrete admixed with microsilica as compared to rice straw ash.

Equation 7.1 shows the reaction between $Ca(OH)_2$ and HCl solution leading to formation of $CaCl_2$, which is a water-soluble salt [346]. In the presence of water, these soluble salts find smooth movement to the outer parts of concretes. Under such a situation, continuous reactions will increase the porosity of cement pastes, and the resultant increase in the pore volume may speed up the rate of reaction [169]. Equation 7.2 shows the reaction of HCl with C-S-H after all of the calcium hydroxide is consumed. In situations where water contains chlorides, and the cement mass is exposed to the acidic pH of the ingressing solution, there is a progressive neutralization of the alkalinity of the cement paste due to calcium dissolution which consequences the dissolving of portlandite and calcium-silicate hydrates (C-S-H) [357].

$$Ca(OH)_2 + 2HCl \rightarrow CaCl_2 + 2H_2O \quad (7.1)$$

$$3CaO{\cdot}2SiO_2{\cdot}3H_2O + 6HCl \rightarrow 3CaCl_2 + 2Si(OH)_4 + 2H_2O \quad (7.2)$$

(aqueous)

In the case of H_2SO_4 attack, the evaluation of reactions can be divided into two parts (Equation 7.3-7.4 and Equation 7.5). In the first stage, deterioration of $Ca(OH)_2$ results in expansive gypsum formation (Equation 7.3). The gypsum then reacts with tri-calcium aluminate (C_3A) in an aqueous environment to form a relatively more expansive ettringite (Equation 7.4) [168]. This expansion causes cracks in concrete. Equation 7.5 shows the reaction of H_2SO_4 with C-S-H in the second stage after all of the calcium hydroxide has been consumed.

$$Ca(OH)_2 + H_2SO_4 \rightarrow \underset{\text{(Gypsum)}}{CaSO_4 \cdot 2H_2O} \qquad 7.3$$

$$3CaSO_4 \cdot 2H_2O + 3CaO \cdot Al_2O_3 + 30H_2O \rightarrow \underset{\text{(Ettringite)}}{3CaO \cdot Al_2O_3 \cdot 3CaSO_4 \cdot 32H_2O} \qquad 7.4$$

$$3CaO \cdot 2SiO_2 \cdot 3H_2O + 3H_2SO_4 \rightarrow \underset{\text{(Gypsum)}}{3CaSO_4 \cdot 2H_2O} + \underset{\text{(aqueous)}}{2Si(OH)_4} \qquad 7.5$$

In this study, HCl was more corrosive to concrete as compared to H_2SO_4 because $CaCl_2$ being soluble in water has the tendency of getting leached out from the surface of concrete thereby making concrete porous [346]. However, gypsum and ettringite (less soluble in water) are formed closer to the concrete surface due to poor penetration capability of H_2SO_4 [331], [358]. Another reason for less susceptibility of concrete to H_2SO_4 could also be due to less amount of C_3A content in cement (primary binder). The lesser C_3A content in the cement may have compromised the transformation of gypsum (less expansive) to ettringite (more expansive). Also, the hydrated silica formed by the reaction between H_2SO_4 and C-S-H gel (Equation 7.5) offers greater protection to the concrete surface as compared to hydrated silica formed by the reaction between HCl and C-S-H gel (Equation 7.2) [152], [359].

The loss of compressive strength of concrete admixed with RSA and MS was lower as compared to the control concrete. For 28 days of water curing and subsequent

HCl immersion, the difference between percentage loss of compressive strength of control concrete (R0) and concrete of other mix (R10, M2.5, M5, M7.5, M10, R5M5, R5M7.5, R10M5 and R10M7.5) was 3.19, 2.56, 3.1, 3.32, 3.71, 3.67, 3.68, 3.8 and 3.86 respectively. The same difference was 3.11, 3.01, 3.04, 3.12, 4.1, 3.86, 3.87, 4.16 and 4.2 respectively for 28 days of water curing and subsequent H_2SO_4 immersion. It was observed that the loss of compressive strength at 365 days of water curing was lower as compared to 28 days of water curing. The loss of compressive strength was least in the concrete mix R10M7.5. Similar to the results of the loss of mass, rice straw ash as compared to microsilica was less effective in lowering the loss of compressive strength due to immersion in acidic solutions.

7.7.3 Visual Observation

Figure 7.10 shows the effects of sulphuric acid attack on concrete admixed with RSA and MS. When H_2SO_4 solution was attacking concrete, gypsum was formed on the vulnerable surface (or exposed surface) of concrete due to its low dissolvability in water and also due to poor penetration capacity of sulphuric acid [331], [358]. The sulphuric acid has poor penetration capacity because formation of gypsum on the concrete surface is quicker than the penetration of sulphate ions (SO_4^{2-}) into the concrete [360]. The expansion in concrete (because of gypsum formation) induces mechanical stresses which eventually lead to microcracks in the hardened cement paste and to spalling of the materials from concrete surface. These phenomena were also observed in the test results of the present study. As can be noticed in Figure 7.10, all the concrete mixes exposed to H_2SO_4 solution for 30 days, had a layer of gypsum (whitish colour) on the surface due to which most of the materials at the surface spalled off. It also led to

microcracks in the microstructure of hardened cementitious paste which were confirmed by the SEM analysis.

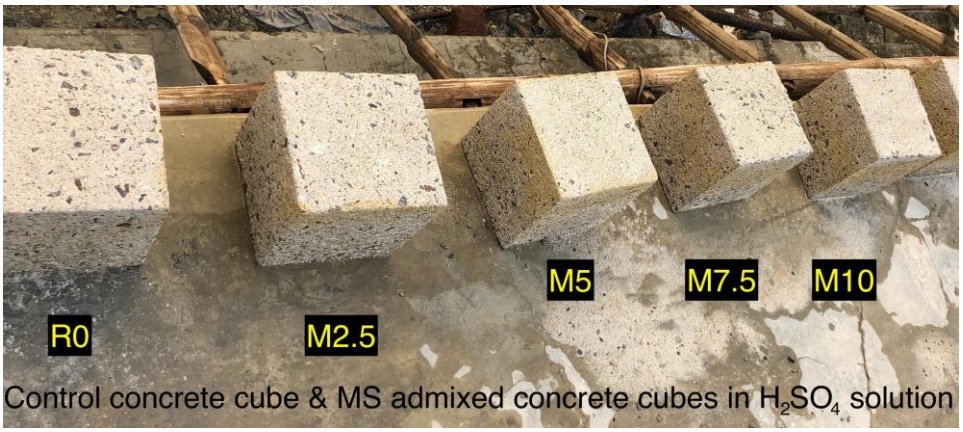

(a)

(b)

Figure 7.10 Cubes of **(a)** control and MS admixed concrete **(b)** RSA admixed and RSA-MS admixed concrete after 28 days of water curing and 30 days in H_2SO_4 solution

Figure 7.11 shows the effects of hydrochloric acid attack on concrete admixed with RSA and MS. When HCl solution was attacking concrete, $CaCl_2$ was formed and owing to its high dissolvability in water, it was able to leach out from the hardened concrete leading to removal of fine aggregates from the cement matrix [152], [350]. However, the outer surfaces of most of the concrete mixes were intact even after being exposed to HCl solution for 30 days. Also, remarkable deterioration was observed on

the edges and corners of the cubes as they are the weakest part of the concrete cubes. It could be the main reason behind the loss of mass in case of HCl attack because unlike H_2SO_4 attack, there was marginal spalling of materials from the surfaces of concrete. However, large size pores were observed on the exposed surfaces which were non-existent in the case of sulphuric acid attack. It confirms that $CaCl_2$ leaches out from concrete which increases the porosity and permeability of concrete, thereby leading to loss of mass and loss of compressive strength [361].

(a)

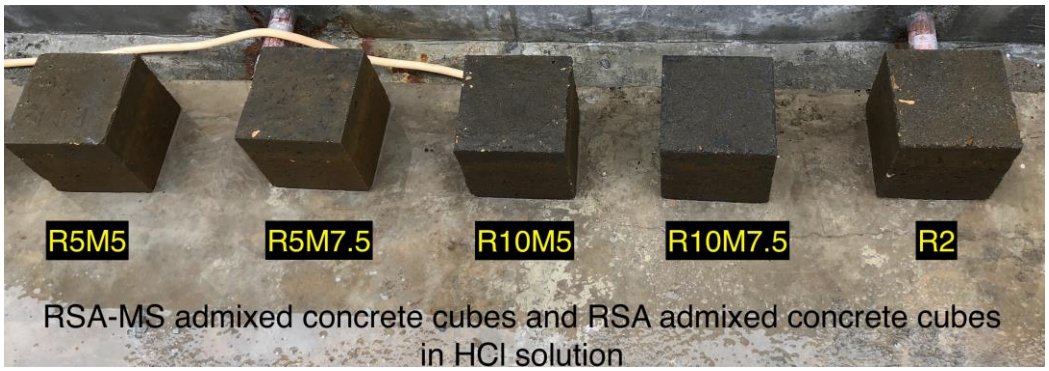

(b)

Figure 7.11 Cubes of **(a)** control and MS admixed concrete **(b)** RSA admixed and RSA-MS admixed concrete after 28 days in water and 30 days in HCl solution

On comparing Figure 7.10 and 7.11, initially, it was perceived that the loss of mass was higher for concrete cubes exposed to H_2SO_4 solution because they had more damaged surface. However, on analysing the actual mass of concrete cubes after an acid attack, it was found that the concrete cubes exposed to HCl had a higher loss of mass. This higher loss of mass could be attributed to the penetration of hydrochloric acid into

concrete and formation of water-soluble salts ($CaCl_2$) which eventually leached out. As loss of mass was higher in case of HCl attack, it can be concluded that remarkable amount of deterioration at edges and corners (HCl attack) was more threatening than spalling of materials from the concrete surface (H_2SO_4 attack).

Figure 7.12 and Figure 7.13 shows the effects of RSA, MS and RSA-MS composite on the resistance of concrete cubes (10% OPC replacement level) to 30 days immersion in acidic solution. It was found in the loss of mass and loss of compressive strength test that concrete admixed with MS was more effective than RSA-MS composite and RSA under acidic immersion. It can be confirmed by visual observation from Figure 7.12 and 7.13. In the case of H_2SO_4 attack, the spalling of materials from the surface of concrete cubes was found to be higher in R10 followed by R5M5 and M10 (Figure 7.12c). As a result, R10 was least resistant to the sulphuric acid attack in comparison with M10 (Figure 7.12a) and R5M5 (Figure 7.12b). Similarly, in the case of HCl attack, the number of pores were higher and the corners and edges were more damaged in mix R10 (Figure 7.13c).

(a)

(b)

(c)

Figure 7.12 Concrete cubes of mix **(a)** M10 (10% MS) **(b)** R5M5 (5% RSA and 5% MS) **(c)** R10 (10% RSA) after 28 days of water curing and 30 days in H_2SO_4 solution

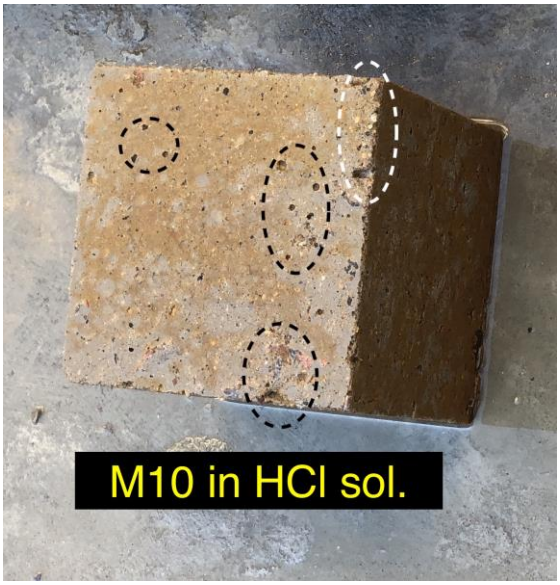

(a)

(b)

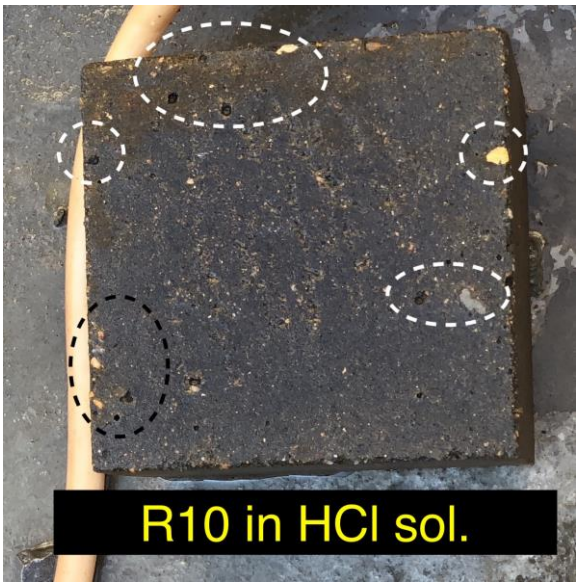

(c)

Figure 7.13 Concrete cubes of mix **(a)** M10 (10% MS) **(b)** R5M5 (5% RSA and 5% MS) **(c)** R10 (10% RSA) after 28 days of water curing and 30 days in HCl solution

7.7.4 Mineralogical Analysis

The mineralogical analysis (by XRD) of the control concrete, as well as concrete admixed with RSA and MS at 365 days of water curing followed by 30 days immersion in HCl and H_2SO_4 solution, is shown in Figure 7.14 and Figure 7.15 respectively. Only 5 mixes, i.e., R0, R10, M7.5, R5M7.5, and R10M7.5, were selected

for XRD analysis. R0 was chosen as it was the control mix while R10 was selected because it was the only mix containing rice straw ash as a mineral admixture. The maximum compressive strength among all the mix tested was observed in M7.5 while maximum compressive strength among the mixes containing a composite of rice straw ash and microsilica was observed in R5M7.5. R10M7.5 had the least percentage loss of mass and compressive strength amongst all the concrete mixes.

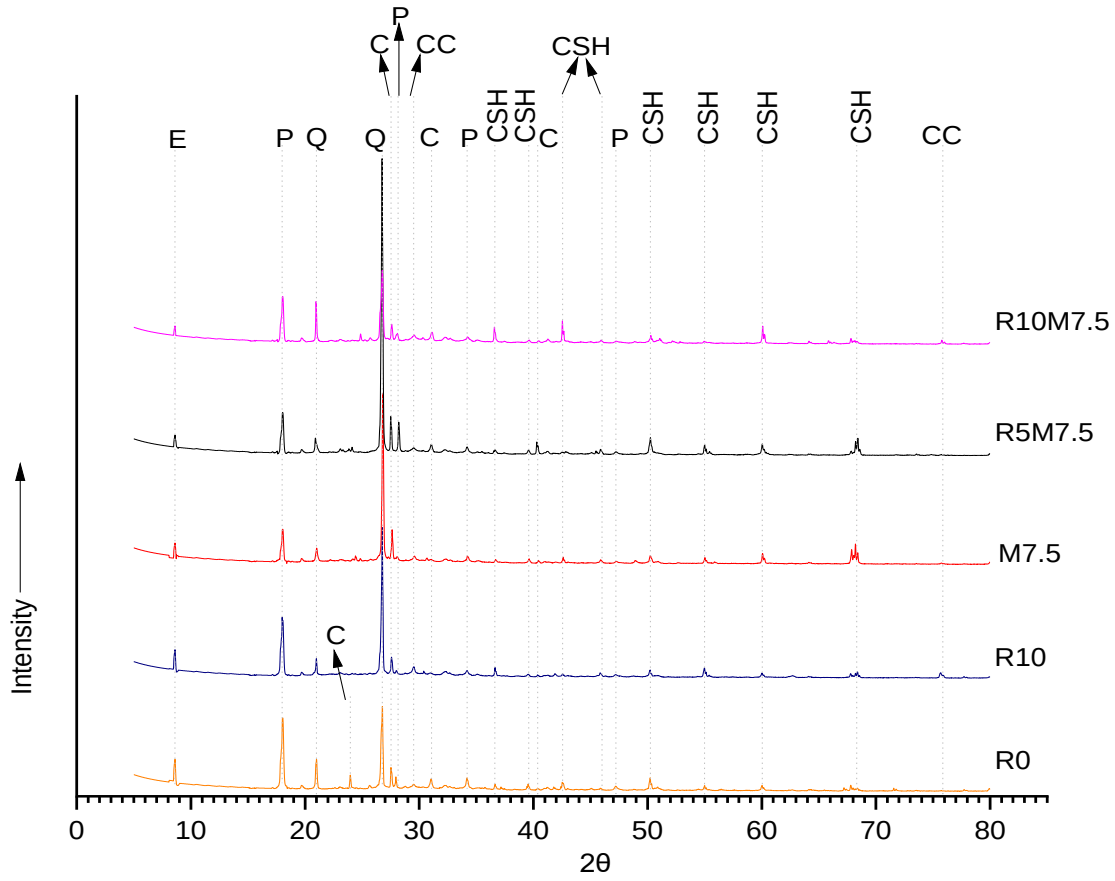

Figure 7.14 XRD analysis of concrete of mix R0, R10, M7.5, R5M7.5 and R10M7.5 at 365 days of water curing and 30 days of HCl immersion

(E – Ettringite; P – Portlandite; Q – Quartz; C – $CaCl_2$; CC – Calcite; CSH – Calcium Silicate Hydrate)

Figure 7.14 shows the diffractograms of the concrete subjected to 365 days of water curing and subsequent 30 days of immersion in HCl solution. The peaks of portlandite ($Ca(OH)_2$) in all the concrete mixes were lower due to dissolution of $Ca(OH)_2$ in HCl solution which eventually led to the formation of $CaCl_2$. The peaks of

$CaCl_2$ had low intensity because of its high solubility in water which is around 279.3g per 100g of water as found in the study by Izquierdo et al. (2016) [362]. It leaches out from the concrete matrix, thereby its identification is difficult in XRD analysis. Also, the surface of the concrete cubes becomes free from calcium salt ($CaCl_2$) due to washing with potable water to remove loose or deposited materials after acidic immersion. The leaching effect of calcium salt significantly affects the loss of mass and loss of compressive strength as given in Table 7.14 and Table 7.17, respectively. The intensity of peaks of portlandite was lower in the concrete of mix R10, M7.5, R5M7.5 and R10M7.5 as compared to R0 because of pozzolanic activity of RSA and MS which resulted in the formation of additional C-S-H gel. However, the formation of additional C-S-H gel increased the vulnerability of the concrete to decomposition in acidic solution as per Equation 7.2. This was the main reason behind higher loss of mass and loss of compressive strength in the concrete of mix M7.5 (Figure 7.7 and Figure 7.9 respectively) as compared to R5M7.5 and R10M7.5 even though M7.5 had the highest compressive strength amongst all the mixes. Therefore, it can be said that when concrete containing highly reactive mineral admixture like MS (for mix M7.5) was subjected to immersion in HCl solution, most of the formation of $CaCl_2$ was due to dissolution of C-S-H gel while in concrete containing composite of RSA and MS (for mix R5M7.5 and R10M7.5), formation of $CaCl_2$ was due to dissolution of C-S-H gel as well as portlandite. The adverse effect of HCl solution was distributed between C-S-H gel and portlandite in the concrete of mix R5M7.5 and R10M7.5, thereby reducing the overall impact of the acidic solution. The peaks of dormant phases of quartz and calcite ($CaCO_3$) were also observed in the XRD diffractograms of the concrete. The presence of calcite could be attributed to the action of atmospheric carbon dioxide [363] while the presence of quartz could be attributed to the presence of fine aggregates, RSA and

MS. The effect of coarse aggregates was ignored as they were separated from hardened cement paste while preparing powdered samples for XRD analysis. The concrete of mix R10, M7.5, R5M7.5 and R10M7.5 exhibited a reduction in the loss of mass and loss of compressive strength as compared to control concrete R0 which can be explained by high-intensity peaks of C-S-H gel and low-intensity peaks of portlandite [362].

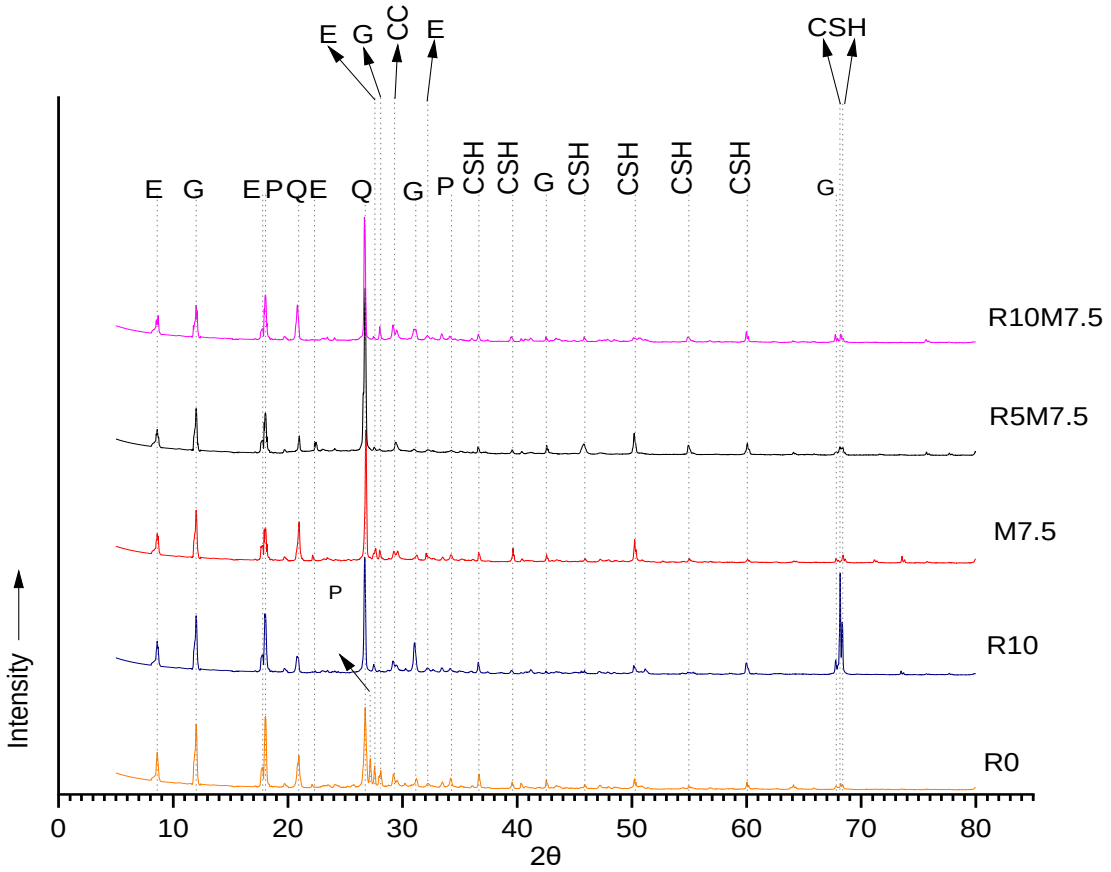

Figure 7.15 XRD analysis of concrete of mix R0, R10, M7.5, R5M7.5 and R10M7.5 at 365 days of water curing and 30 days of H_2SO_4 immersion

(E – Ettringite; G – Gypsum; P – Portlandite; Q – Quartz; CC – Calcite; CSH – Calcium Silicate Hydrate)

Figure 7.15 shows the diffractograms of the concrete subjected to 365 days of water curing and subsequent 30 days of immersion in H_2SO_4 solution. The dissolution of $Ca(OH)_2$ in H_2SO_4 solution led to the formation of a whitish layer of gypsum on the concrete surface (Figure 7.10). The peaks of gypsum had high intensity due to its low solubility in water which is around 0.24g per 100g of water as found in the study by

Izquierdo et al. (2016) [362]. The presence of MS and RSA reduces the $Ca(OH)_2$ content in the concrete, which can be corroborated by the low-intensity peaks of portlandite in Figure 7.15. Similar to the reasons given in the preceding paragraph, the decalcification of additional C-S-H gel (due to pozzolanic activity) in the concrete of mix M7.5 was responsible for higher loss of mass as well as compressive strength in comparison with the concrete of mix R5M7.5 and R10M7.5. The peaks of portlandite in the concrete of mix R0, R10, M7.5, R5M7.5 and R10M7.5 were similar in both the acidic solutions. Similar to the results of immersion in HCl solution, few peaks of quartz and calcite ($CaCO_3$) were also observed in the XRD analysis of concrete in H_2SO_4 solution. Few peaks of ettringite were also found; however, they were limited to low-intensity because of the masking effect of other governing phases like gypsum. Gypsum causes microcracks in the hardened cement paste due to its expansive nature; however, most of the concrete matrix remains intact.

7.7.5 Microstructural Analysis

Figure 7.16 shows the SEM images of the concrete subjected to 365 days of water curing and subsequent 30 days of immersion in HCl solution. The hydrated compounds of C-S-H and $Ca(OH)_2$ having characteristically porous appearance composing of flakes or flattened equant grains growing together were observed in control concrete R0 (Figure 7.16a). $Ca(OH)_2$ reacts with HCl to form $CaCl_2$ which due to its high solubility in water makes concrete tenuous. It can be seen that the microstructure of control concrete R0 under HCl solution (Figure 7.16a) has a highly tenuous surface texture as compared to concrete admixed with RSA and MS. Also, significant amounts of precipitated salts were observed in control concrete R0. Micrograph of the control concrete R0 is marked by the presence of large voids while

the number of voids was considerably reduced in other mixes. The consumption of $Ca(OH)_2$ and the formation of additional C-S-H gel during the pozzolanic reaction was the main reason behind reduction in the number of voids. The compressive strength of concrete when exposed to HCl solution was highest for mix M7.5, which was due to comparatively denser concrete matrix as can be seen in Figure 7.16c. However, large size pores/cavities were observed in M7.5. The reaction between acidic solution and C-S-H gel led to the formation of $CaCl_2$, which leached out from the surface of concrete and weakened the bond between aggregates and hardened cement paste. These pores may have been caused due to separation of aggregates, which can be corroborated by higher loss of mass as well as compressive strength in the concrete of mix M7.5 as compared to R5M7.5 and R10M7.5. Also, higher amount of C-S-H gel was observed in the concrete of mix R5M7.5 and R10M7.5 (Figure 7.16d and e respectively) as compared to M7.5 even though MS is more pozzolanic as compared to RSA. It corroborates the results of XRD analysis that the higher loss of mass in M7.5 was due to reaction between C-S-H gel and HCl solution while the detrimental effect of HCl solution on R5M7.5 and R10M7.5 was distributed between C-S-H gel and portlandite present in the hardened cement paste. Remains of partially reacted MS were also observed in the concrete of mix M7.5.

Figure 7.17 shows the SEM images of the concrete subjected to 365 days of water curing and subsequent 30 days of immersion in H_2SO_4 solution. Large scale propagation of micro-cracks was observed in control concrete R0 (Figure 7.17a) as compared to concrete admixed with RSA and MS. The degree of corrosive action of H_2SO_4 solution can be distinguished by the presence of microcracks travelling into the concrete. Formation of the micro-cracks was due to the expansive nature of gypsum and ettringite (reaction products of H_2SO_4 solution and hydration products). In any case, the

concrete admixed with RSA and MS demonstrated the best ability to opposing the propagation of micro-cracks. The fact that not many micro-cracks were observed which could be credited to the dense pore structure of RSA and MS concrete that counteracts the ingress of sulphate ions; thus preventing the formation of ettringite and gypsum. Similar to the observations of HCl attack, the loss of mass, as well as compressive strength in the concrete of mix M7.5 under H_2SO_4 immersion, was higher as compared to R5M7.5 and R10M7.5 even though the microstructure of M7.5 was denser than other mixes as observed in Figure 7.17c. The lower compressive strength of R5M7.5 and R10M7.5 as compared to M7.5 under acidic solution could be attributed to the presence of voids as the strength of concrete is influenced by the volume of voids in concrete. In comparison to gypsum and ettringite, formation of $CaCl_2$ seems to be the major concern for dissolution of hydrated cement paste and consequently causes higher percentage loss of mass and percentage loss of compressive strength.

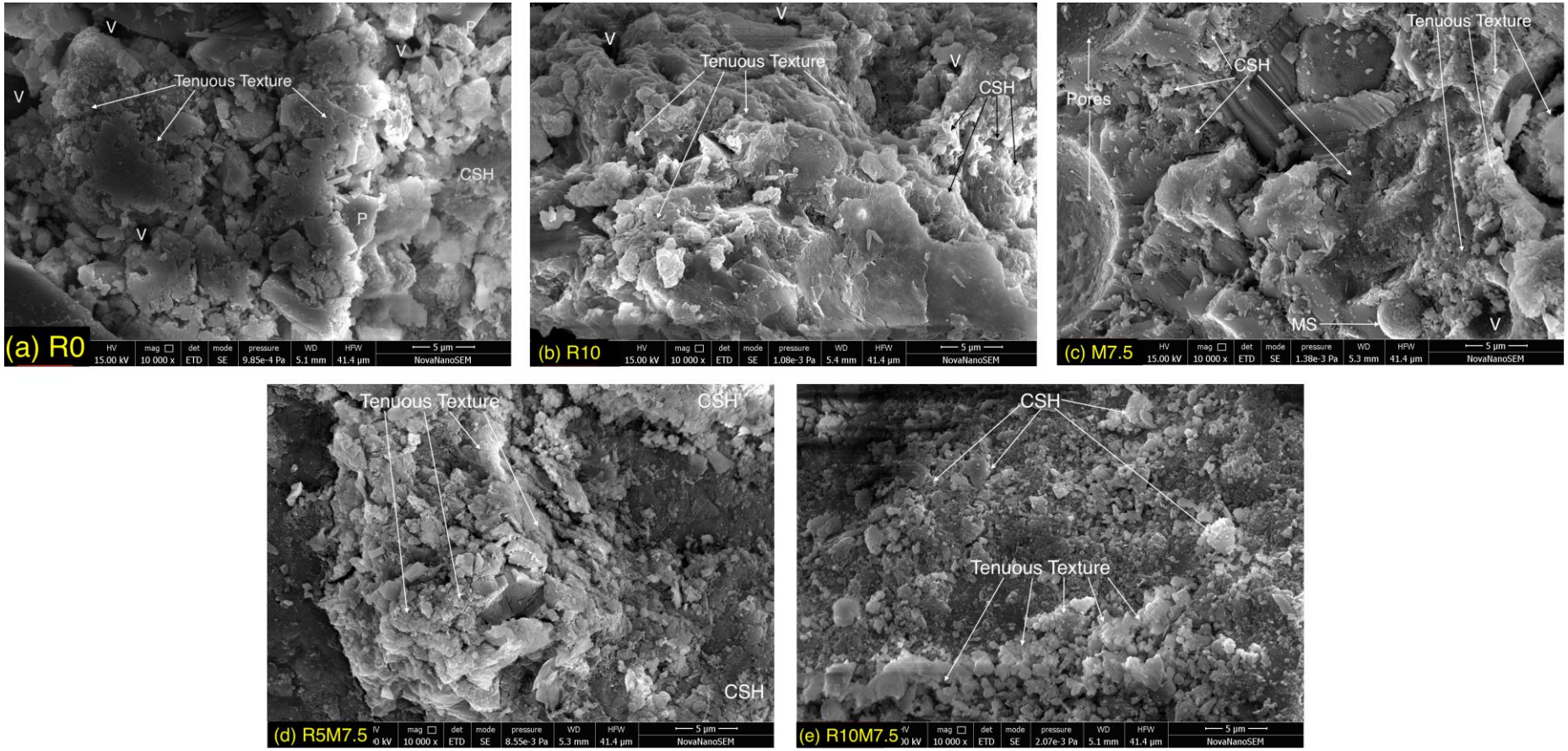

Figure 7.16 SEM micrographs of concrete of mix **(a)** R0 **(b)** R10 **(c)** M7.5 **(d)** R5M7.5 **(e)** R10M7.5 at 365 days of water curing and 30 days of HCl immersion

(V – Voids, P – Portlandite, CSH – Calcium Silicate Hydrate)

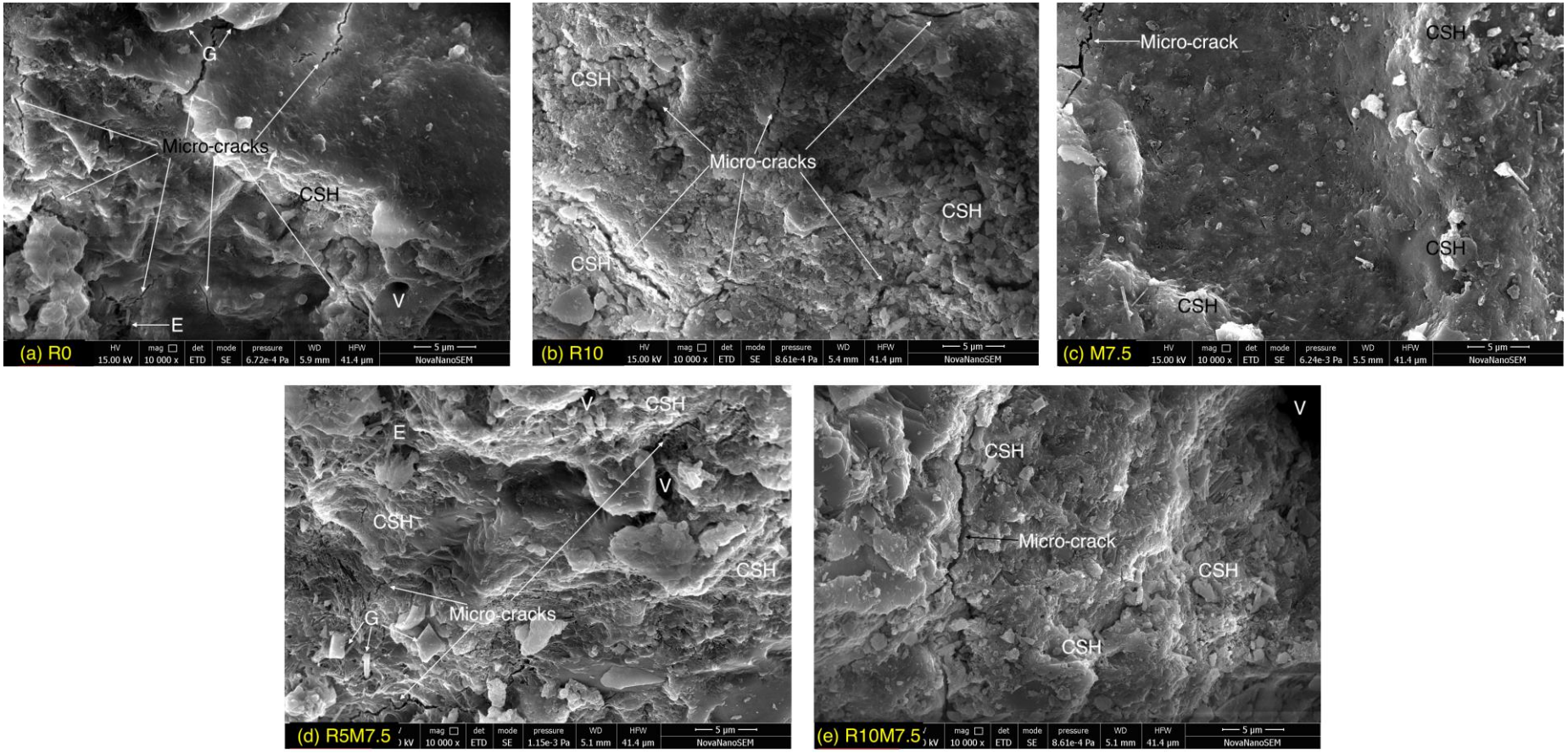

Figure 7.17 SEM micrographs of concrete of mix **(a)** R0 **(b)** R10 **(c)** M7.5 **(d)** R5M7.5 **(e)** R10M7.5 at 365 days of water curing and 30 days of H_2SO_4 immersion

(V – Voids, G – Gypsum, E – Ettringite, CSH – Calcium Silicate Hydrate)

7.8 EFFECTS OF ACCELERATED CARBONATION CURING

Carbonation of concrete takes place when it is exposed to carbon dioxide (CO_2). The exposure of concrete to the acidic environment or CO_2 from the atmosphere affects its physical and chemical properties [364]. The effects of accelerated carbonation curing (ACC) on strength and carbonation depth of concrete admixed with RSA and MS are given in the subsequent sections.

7.8.1 Mechanical Strength

The compressive, flexural and split tensile strength of concrete at 28 days of water curing as well as 28 days of combined curing (14 days water curing + 14 days ACC) are given in Table 7.18 and shown in Figure 7.18. The percentage increase in the compressive, flexural and split tensile strength of concrete due to 28 days of combined curing w.r.t respective strengths at 28 days of water curing are given in Table 7.19.

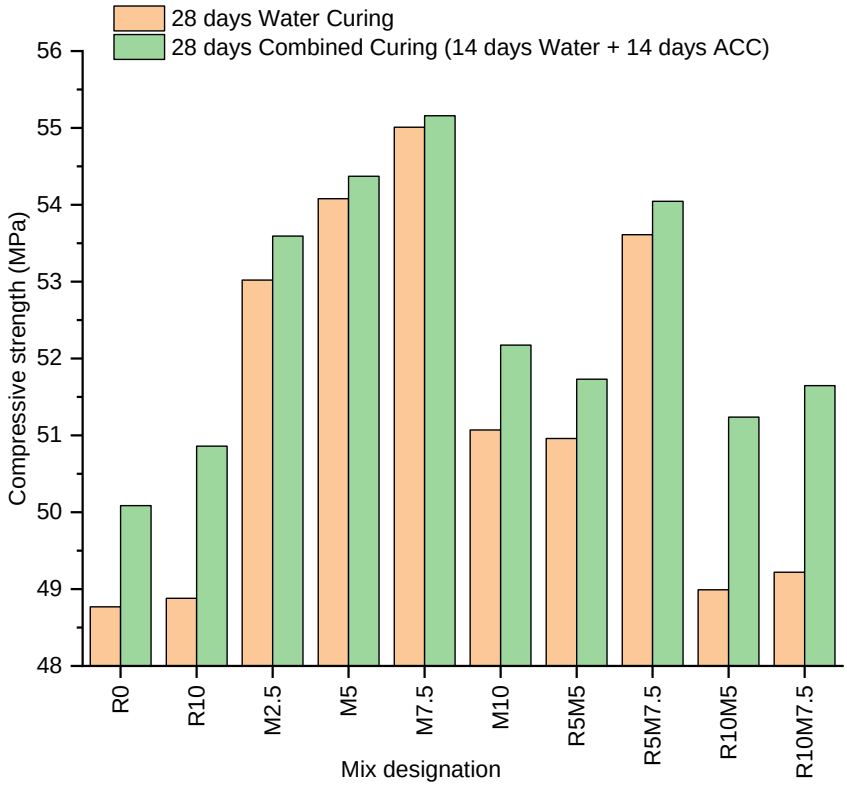

(a) Compressive strength

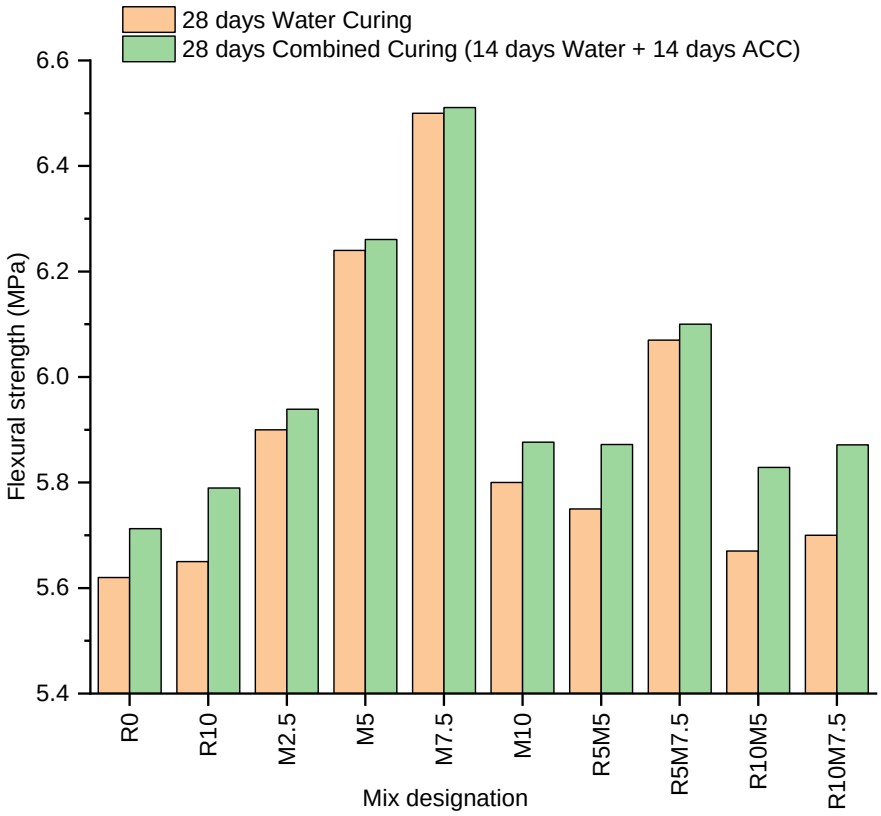

(b) Flexural strength

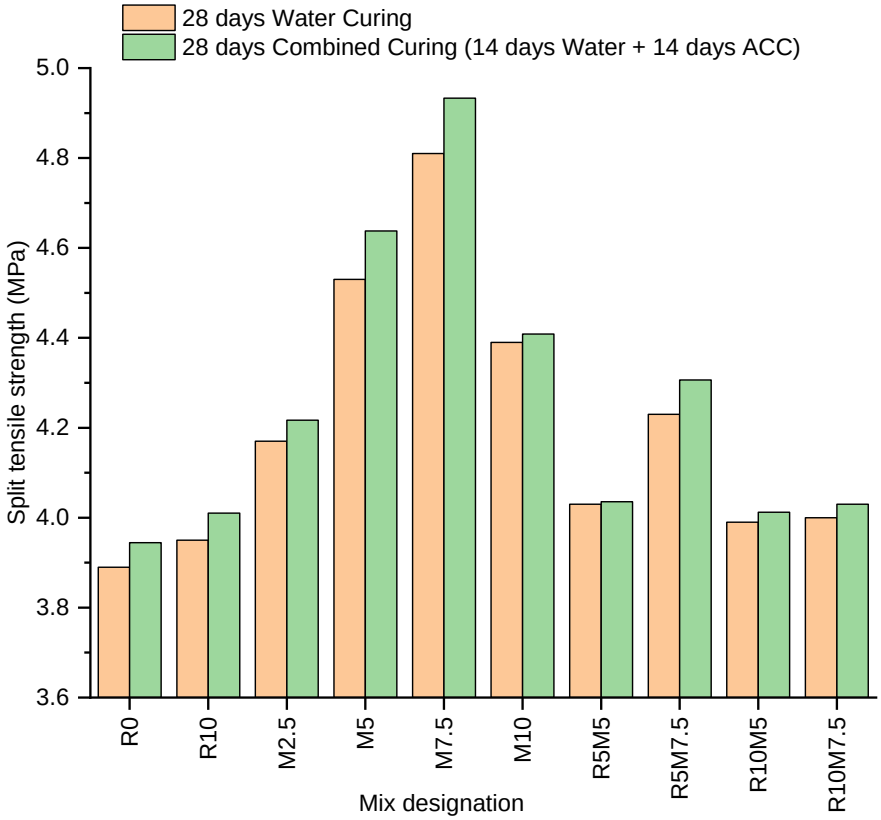

(c) Split tensile strength

Figure 7.18 Graphs showing the effect of accelerated carbonation curing on **(a)** Compressive strength **(b)** Flexural strength **(c)** Split tensile strength

The mechanical strengths of concrete admixed with RSA and MS were higher in case of 28 days of combined curing as compared to 28 days of water curing (Table 7.18). As per the literature, higher strength due to ACC may be attributed to the formation of $CaCO_3$, which reduces the porosity of the concrete matrix [153], [179], [313]. The percentage increase in the compressive strength of concrete mix R0, R10, M2.5, M5, M7.5, M10, R5M5, R5M7.5, R10M5, and R10M7.5 at 28 days of combined curing w.r.t 28 days of water curing was 2.7%, 4.05%, 1.08%, 0.54%, 0.27%, 2.16%, 1.51%, 0.81%, 4.59%, and 4.93% respectively (Table 7.19). The percentage increase in the flexural and split tensile strength for the same was 1.65%, 2.47%, 0.66%, 0.33%, 0.16%, 1.32%, 2.12%, 0.49%, 2.80%, 3.01% respectively and 1.4%, 1.52%, 1.12%, 2.38%, 2.56%, 0.42%, 0.14%, 1.8%, 0.56%, 0.75% respectively (Table 7.19). As observed in Table 7.19, the percentage increase in compressive and flexural strength was mostly higher in concrete admixed with RSA (with or without microsilica) and was maximum in the concrete of mix R10M7.5. The percentage increase in split tensile strength was mostly higher in concrete admixed with MS and was maximum in the concrete of mix M7.5. Higher strength of concrete admixed with RSA and MS due to carbonation was because of the combined impact of additional C-S-H formation as well as $CaCO_3$ formation. $CaCO_3$ occupies more space as compared to $Ca(OH)_2$ leading to denser concrete matrix.

Table 7.18 Various strength of concrete at 28 days of water curing and 28 days of combined curing (14 days water + 14 days ACC)

Mix	Compressive Strength (MPa)		Flexural Strength (MPa)		Split Tensile Strength (MPa)	
	Water Curing	Combined Curing	Water Curing	Combined Curing	Water Curing	Combined Curing
R0	48.77	50.09	5.62	5.71	3.89	3.94
R10	48.88	50.86	5.65	5.79	3.95	4.01
M2.5	53.02	53.59	5.9	5.94	4.17	4.22
M5	54.08	54.37	6.24	6.26	4.53	4.64
M7.5	55.01	55.16	6.5	6.51	4.81	4.93
M10	51.07	52.17	5.8	5.88	4.39	4.41
R5M5	50.96	51.73	5.75	5.87	4.03	4.04
R5M7.5	53.61	54.04	6.07	6.10	4.23	4.31
R10M5	48.99	51.24	5.67	5.83	3.99	4.01
R10M7.5	49.22	51.65	5.7	5.87	4	4.03

Table 7.19 Percentage increase in strength of concrete due to 28 days of combined curing w.r.t. 28 days of water curing

Mix	R0	R10	M2.5	M5	M7.5	M10	R5M5	R5M7.5	R10M5	R10M7.5
Increase in Compressive Strength (%)	2.7	4.05	1.08	0.54	0.27	2.16	1.51	0.81	4.59	4.93
Increase in Flexural Strength (%)	1.65	2.47	0.66	0.33	0.16	1.32	2.12	0.49	2.8	3.01
Increase in Split Tensile Strength (%)	1.4	1.52	1.12	2.38	2.56	0.42	0.14	1.8	0.56	0.75

The high concentration of carbon dioxide isn't necessarily required for obtaining a high degree of carbonation curing. In general, CO_2 reacts directly with C_3S and C_2S in the absence of $Ca(OH)_2$ to form calcium carbonate in accelerated carbonation of concrete (Equation 7.6 and 7.7 respectively) [365], [366]. It may be attributed to the immediate ACC of concrete samples (a few hours of preconditioning) after 24 hours of casting. Therefore the carbonation of hydration products (such as C-S-H and $Ca(OH)_2$ as per Equation 7.8 and 7.9 respectively) may be ignored due to the absence of sufficient moisture required for their formation [249]. When cement paste is admixed with silica-rich mineral admixtures, the $Ca(OH)_2$ content of the paste decreases significantly because most of it takes part in the pozzolanic reaction by mineral admixtures. As a result, the carbonation of $Ca(OH)_2$ reduces significantly and less amount of $CaCO_3$ is formed in the admixed concrete (as per Equation 7.9). Due to fewer amounts of tricalcium aluminate (C_3A) and tetracalcium aluminoferrite (C_4AF) in the cement, their reaction with CO_2 in the process of carbonation can also be ignored [249], [367].

$$3CaO.SiO_2\,(C_3S) + 3CO_2 + H_2O \rightarrow SiO_2.H_2O\ (\text{silica gel}) + 3CaCO_3 \qquad 7.6$$

$$2CaO.SiO_2\,(C_2S) + 2CO_2 + H_2O \rightarrow SiO_2.H_2O\ (\text{silica gel}) + 2CaCO_3 \qquad 7.7$$

$$3CaO.2SiO_2.3H_2O + 3CO_2 \rightarrow 3CaCO_3 + 2SiO_2.3H_2O \qquad 7.8$$

$$Ca(OH)_2 + CO_2 \rightarrow CaCO_3 + H_2O \qquad 7.9$$

The compounds of calcium silicate (C_3S or C_2S, present in cement) are mainly responsible for strength development in concrete. They liberate C-S-H and $Ca(OH)_2$ on reaction with water. Usually, concrete achieves 65-70% and 90-95% strength at 7 and

28 days of water curing respectively in comparison to strength at 365 days of curing [368]. In other words, the majority of the calcium silicate compounds (in the presence of water) transform into various hydration products up to 28 days of curing. However, in the current study, various mixes of concrete were subjected to only 14 days of water curing which prevented the complete transformation of calcium silicate compounds into C-S-H and $Ca(OH)_2$. Moreover, $Ca(OH)_2$ formed due to 14 days of water curing was consumed by pozzolanic action of RSA and MS, resulting in the formation of additional C-S-H gel. Therefore, it can be assumed that negligible amount of $Ca(OH)_2$ was present in concrete before the start of ACC in a carbonation chamber. Consequently, it can be concluded that CO_2 reacted directly with C_3S and C_2S to form $CaCO_3$ as per Equation 7.6 and Equation 7.7 respectively (as per the study by Hussain et al. (2017) [153], carbonation of C-S-H is extremely slow and can be ignored). However, the complete conversion of C_3S and C_2S into $CaCO_3$ during ACC is not possible because as the time progresses, $CaCO_3$ forms a dense layer around the cementitious particles stopping their further carbonation [369]–[371].

7.8.2 Carbonation Depth

The depth of carbonation in the concrete of all the mix is shown in Figure 7.19. It also shows the compressive strength of the respective mix at 28 days of combined curing. The carbonation depth was lower in concrete admixed with rice straw ash and microsilica as compared to control concrete. It was because the size and volume of the pores in the admixed concrete were reduced due to the filler and pozzolanic effect of the mineral admixtures [179]. This decrease in carbonation rate was in agreement with the study of few researchers [179], [180] while some researchers showed heightened carbonation rate in concrete due to admixing of mineral admixtures like fly ash,

metakaolin, limestone, pulverized fuel ash, etc. [153], [181], [182]. For admixed concrete, the carbonation depth was minimum in mix M7.5 (1 mm) and maximum in mix R10 (17 mm) as shown in Figure 7.20. Therefore it can be said that the depth of carbonation was higher in concrete admixed with rice straw ash as compared to microsilica. The ultra-fine particles of MS and their high silica content were the main reasons behind the reduced depth of carbonation in concrete admixed with MS.

The correlation between the depth of carbonation and compressive strength of concrete of all the mix can also be seen in Figure 7.19. It shows that compressive strength increases with decrease in the carbonation depth. This phenomenon has all the earmarks of being reasonable as the size and volume of the pores are the dominating factors in compressive strength and carbonation of concrete [179], [344].

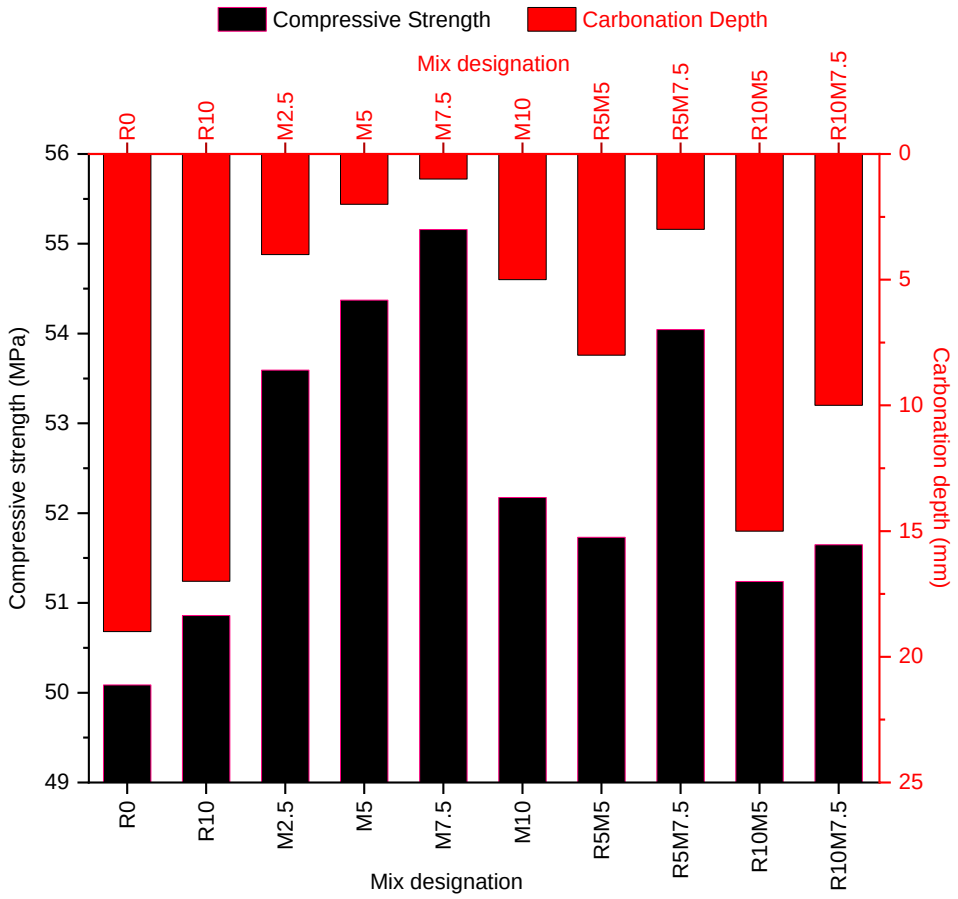

Figure 7.19 Comparison of carbonation depth and compressive strength at 28 days of combined curing

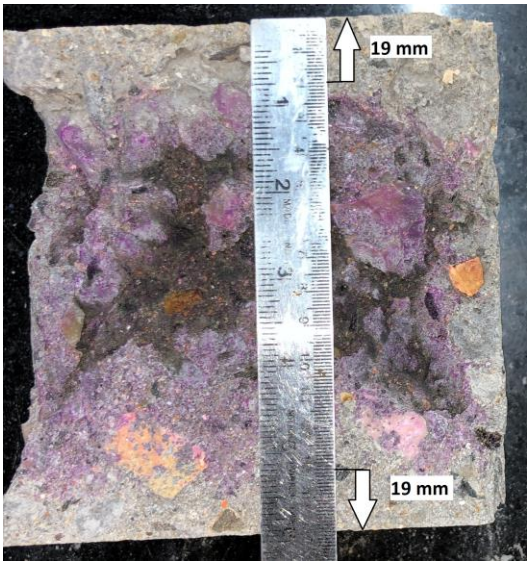

(a) R0

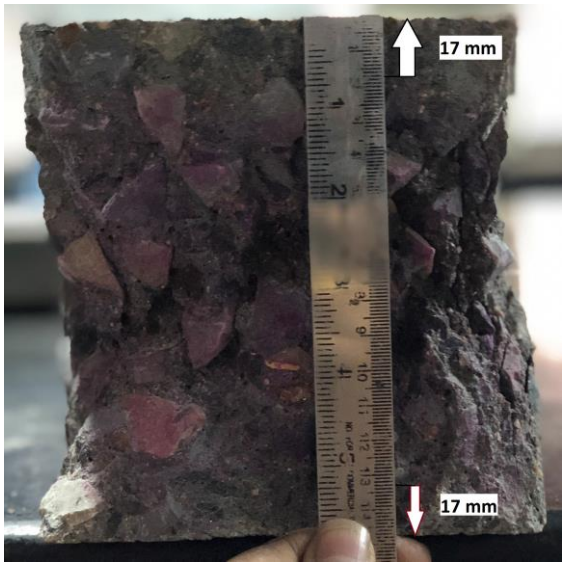

(b) R10

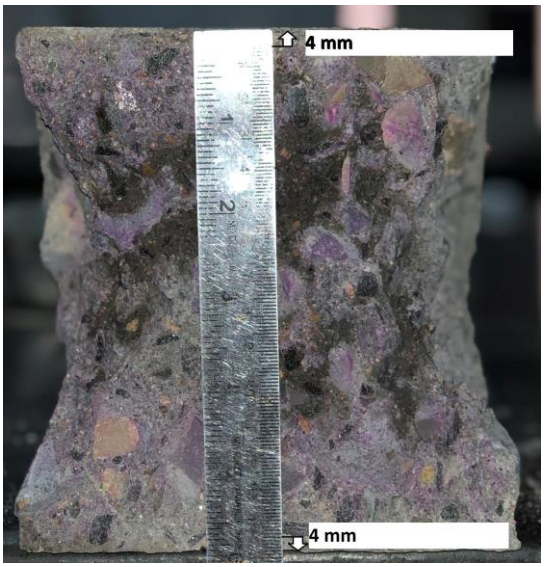

(c) M2.5

(d) M5

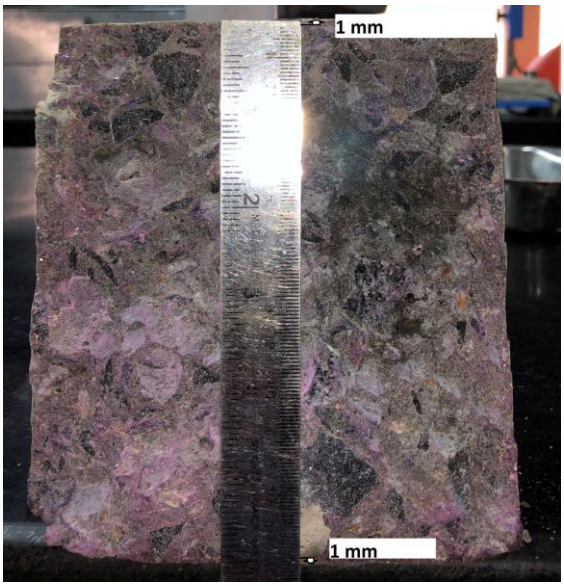

(e) M7.5

(f) M10

(g) R5M5

(h) R5M7.5

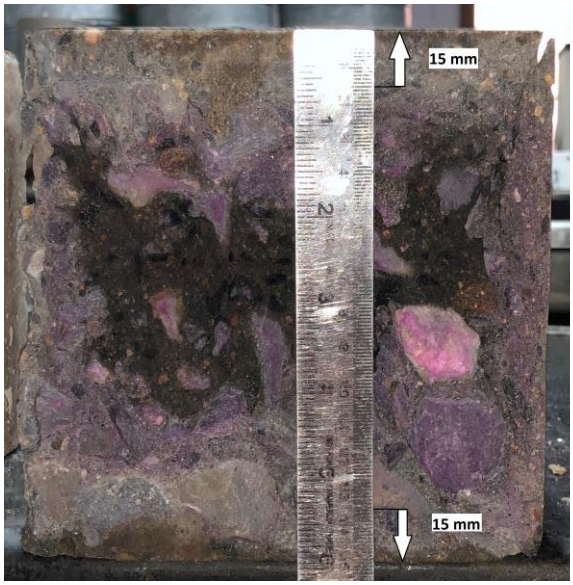

(i) R10M5

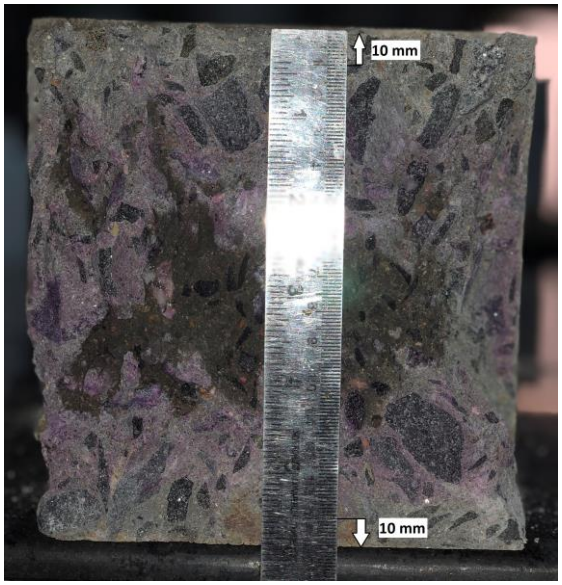

(j) R10M7.5

Figure 7.20 Depth of carbonation in concrete of mix **(a)** R0 **(b)** R10 **(c)** M2.5 **(d)** M5 **(e)** M7.5 **(f)** M10 **(g)** R5M5 **(h)** R5M7.5 **(i)** R10M5 **(j)** R10M7.5

7.9 PREDICTION MODELS

Various equations between different parameters were developed by regression analysis from ORIGIN 2019 software based on the findings of experimental studies.

7.9.1 Saturated Water Absorption

Saturated water absorption of concrete of various mixes was dependent on the age of curing. Therefore, the mathematical relationship between them was described by a power equation in the form of Equation 7.10, with a high coefficient of determination (R^2). The power equations of different concrete mix are given in Table 7.20. These equations were derived from the experimental data given in Table 7.2.

$$f(x) = a \times x^b \qquad 7.10$$

where, $f(x)$ = Saturated water absorption (%),
a, b = constants,
x = curing age (days)

Table 7.20 Mathematical relation between saturated water absorption ('y') and curing age ('x')

Mix	Prediction Models	R^2	Validity
R0	$y = 4.9702 \times x^{-0.124}$	0.9757	$365 \geq x \geq 3$
R10	$y = 4.2088 \times x^{-0.102}$	0.9253	$365 \geq x \geq 3$
M2.5	$y = 4.4695 \times x^{-0.109}$	0.9447	$365 \geq x \geq 3$
M5	$y = 4.3502 \times x^{-0.105}$	0.9428	$365 \geq x \geq 3$
M7.5	$y = 3.9775 \times x^{-0.097}$	0.9271	$365 \geq x \geq 3$
M10	$y = 3.6778 \times x^{-0.144}$	0.9458	$365 \geq x \geq 3$
R5M5	$y = 4.1918 \times x^{-0.154}$	0.9761	$365 \geq x \geq 3$
R5M7.5	$y = 4.0278 \times x^{-0.153}$	0.9802	$365 \geq x \geq 3$
R10M5	$y = 3.6319 \times x^{-0.152}$	0.9682	$365 \geq x \geq 3$
R10M7.5	$y = 3.4336 \times x^{-0.149}$	0.9732	$365 \geq x \geq 3$

7.9.2 Rate of Water Absorption

The power equations between curing age ('x' in days) and the rate of water absorption ('y_s' for secondary and 'y_i' for initial) of each concrete mix were developed by regression analysis with a high coefficient of determination (R^2) as shown in Table 7.21 and Table 7.22. These equations were derived from the experimental data given in Table 7.4 and Table 7.5.

Table 7.21 Mathematical relation between the initial rate of water absorption ('y_i') and curing age ('x')

Mix	Prediction Models	R^2	Validity
R0	$y_i = 14.089 \times x^{-0.206}$	0.8689	$365 \geq x \geq 3$
R10	$y_i = 11.401 \times x^{-0.183}$	0.8935	$365 \geq x \geq 3$
M2.5	$y_i = 13.045 \times x^{-0.194}$	0.8511	$365 \geq x \geq 3$
M5	$y_i = 13.155 \times x^{-0.204}$	0.8696	$365 \geq x \geq 3$
M7.5	$y_i = 9.6023 \times x^{-0.151}$	0.9008	$365 \geq x \geq 3$
M10	$y_i = 7.6106 \times x^{-0.118}$	0.9669	$365 \geq x \geq 3$
R5M5	$y_i = 9.4646 \times x^{-0.155}$	0.9304	$365 \geq x \geq 3$
R5M7.5	$y_i = 7.9986 \times x^{-0.122}$	0.9649	$365 \geq x \geq 3$
R10M5	$y_i = 6.2511 \times x^{-0.085}$	0.8401	$365 \geq x \geq 3$
R10M7.5	$y_i = 14.089 \times x^{-0.206}$	0.9689	$365 \geq x \geq 3$

Table 7.22 Mathematical relation between the secondary rate of water absorption ('y_s') and curing age ('x')

Mix	Prediction Models	R^2	Validity
R0	$y_s = 1.3825 \times x^{-0.202}$	0.8874	$365 \geq x \geq 3$
R10	$y_s = 0.9069 \times x^{-0.148}$	0.917	$365 \geq x \geq 3$
M2.5	$y_s = 1.2867 \times x^{-0.196}$	0.8513	$365 \geq x \geq 3$
M5	$y_s = 1.0801 \times x^{-0.17}$	0.8707	$365 \geq x \geq 3$
M7.5	$y_s = 0.6673 \times x^{-0.095}$	0.939	$365 \geq x \geq 3$
M10	$y_s = 0.5149 \times x^{-0.092}$	0.8813	$365 \geq x \geq 3$
R5M5	$y_s = 0.5983 \times x^{-0.101}$	0.8802	$365 \geq x \geq 3$
R5M7.5	$y_s = 0.5871 \times x^{-0.108}$	0.9162	$365 \geq x \geq 3$
R10M5	$y_s = 0.4767 \times x^{-0.081}$	0.8739	$365 \geq x \geq 3$
R10M7.5	$y_s = 0.4630 \times x^{-0.087}$	0.9454	$365 \geq x \geq 3$

For each concrete mix, one linear equation between the secondary rate of water absorption ('y_s' in 10^{-6} m/s$^{0.5}$) and the initial rate of water absorption ('y_i' in 10^{-6} m/s$^{0.5}$) was developed by regression analysis with very high coefficient of determination (R^2) as shown in Table 7.23.

Table 7.23 Mathematical relation between the secondary ('y_s') and initial rate of water absorption ('y_i')

Mix	Prediction Models	R^2	Validity
R0	$y_s = 0.0955 \times y_i + 0.0267$	0.9992	$365 \geq y_i \geq 3$
R10	$y_s = 0.0687 \times y_i + 0.1229$	0.9902	$365 \geq y_i \geq 3$
M2.5	$y_s = 0.0997 \times y_i + 0.0104$	0.997	$365 \geq y_i \geq 3$
M5	$y_s = 0.0729 \times y_i + 0.1228$	0.9793	$365 \geq y_i \geq 3$
M7.5	$y_s = 0.0491 \times y_i + 0.1979$	0.9486	$365 \geq y_i \geq 3$
M10	$y_s = 0.0498 \times y_i + 0.1215$	0.8322	$365 \geq y_i \geq 3$
R5M5	$y_s = 0.0451 \times y_i + 0.1694$	0.766	$365 \geq y_i \geq 3$
R5M7.5	$y_s = 0.0674 \times y_i + 0.05$	0.8876	$365 \geq y_i \geq 3$
R10M5	$y_s = 0.0693 \times y_i + 0.037$	0.9423	$365 \geq y_i \geq 3$
R10M7.5	$y_s = 0.0581 \times y_i + 0.1125$	0.93	$365 \geq y_i \geq 3$

One linear equation (valid for all concrete mix at all curing age) between the secondary rate of water absorption ('y_s' in 10^{-6} m/s$^{0.5}$) and the initial rate of water absorption ('y_i' in 10^{-6} m/s$^{0.5}$) was developed by regression analysis as shown in Equation 7.11 (R^2 = 0.8791).

$$y_s = 0.0892 \times y_i - 0.02 \qquad (y_i > 0.225) \qquad 7.11$$

7.9.3 Coefficient of Water Absorption

The power equations between the coefficient of water absorption ('y_c' in 10^{-10} m^2/s) and days of curing in water ('x') were developed by regression analysis as shown in Table 7.24. These equations were derived from the experimental data (Table 7.8).

Table 7.24 Mathematical relation between the coefficient of water absorption ('y_c') and days of curing ('x')

Mix	Prediction Models	R^2	Validity
R0	$y_c = 9.7027 \times x^{-0.14}$	0.9391	$365 \geq x \geq 3$
R10	$y_c = 7.6635 \times x^{-0.333}$	0.9144	$365 \geq x \geq 3$
M2.5	$y_c = 9.5402 \times x^{-0.198}$	0.8996	$365 \geq x \geq 3$
M5	$y_c = 8.733 \times x^{-0.318}$	0.8883	$365 \geq x \geq 3$
M7.5	$y_c = 4.7468 \times x^{-0.246}$	0.9349	$365 \geq x \geq 3$
M10	$y_c = 3.1543 \times x^{-0.227}$	0.9664	$365 \geq x \geq 3$
R5M5	$y_c = 3.9606 \times x^{-0.241}$	0.9697	$365 \geq x \geq 3$
R5M7.5	$y_c = 3.651 \times x^{-0.253}$	0.9782	$365 \geq x \geq 3$
R10M5	$y_c = 3.2817 \times x^{-0.275}$	0.9766	$365 \geq x \geq 3$
R10M7.5	$y_c = 2.9015 \times x^{-0.342}$	0.9534	$365 \geq x \geq 3$

7.9.4 Chloride Ion Penetration

The power equations between the chloride percentage at both depths ('y_{10}' for 10-20 mm and 'y_{25}' for 25-35 mm) and days of curing ('x') were developed by regression analysis as shown in Table 7.25 and Table 7.26. These equations were derived from the experimental data given in Table 7.10 and Table 7.11.

Table 7.25 Mathematical relation between chloride percentage at 10-20 mm depth ('y_{10}') & days of curing ('x')

Mix	Prediction Models	R^2	Validity
R0	$y_{10} = 1.6326 \times x^{-0.181}$	0.7886	$365 \geq x \geq 3$
R10	$y_{10} = 1.4592 \times x^{-0.201}$	0.8479	$365 \geq x \geq 3$
M2.5	$y_{10} = 1.5202 \times x^{-0.176}$	0.7854	$365 \geq x \geq 3$
M5	$y_{10} = 1.5258 \times x^{-0.203}$	0.8416	$365 \geq x \geq 3$
M7.5	$y_{10} = 1.4323 \times x^{-0.213}$	0.8566	$365 \geq x \geq 3$
M10	$y_{10} = 1.2497 \times x^{-0.27}$	0.9611	$365 \geq x \geq 3$
R5M5	$y_{10} = 1.2327 \times x^{-0.219}$	0.8109	$365 \geq x \geq 3$
R5M7.5	$y_{10} = 1.1152 \times x^{-0.207}$	0.8248	$365 \geq x \geq 3$
R10M5	$y_{10} = 1.3326 \times x^{-0.344}$	0.9683	$365 \geq x \geq 3$
R10M7.5	$y_{10} = 1.255 \times x^{-0.357}$	0.9507	$365 \geq x \geq 3$

Table 7.26 Mathematical relation between chloride percentage at 25-35 mm depth ('y_{25}') & days of curing ('x')

Mix	Prediction Models	R^2	Validity
R0	$y_{25} = 1.5928 \times x^{-0.185}$	0.8	$365 \geq x \geq 3$
R10	$y_{25} = 1.4785 \times x^{-0.213}$	0.8879	$365 \geq x \geq 3$
M2.5	$y_{25} = 1.533 \times x^{-0.2}$	0.8288	$365 \geq x \geq 3$
M5	$y_{25} = 1.5057 \times x^{-0.204}$	0.8464	$365 \geq x \geq 3$
M7.5	$y_{25} = 1.3171 \times x^{-0.198}$	0.8426	$365 \geq x \geq 3$
M10	$y_{25} = 1.2546 \times x^{-0.284}$	0.9744	$365 \geq x \geq 3$
R5M5	$y_{25} = 1.1717 \times x^{-0.216}$	0.8255	$365 \geq x \geq 3$
R5M7.5	$y_{25} = 1.2316 \times x^{-0.26}$	0.9566	$365 \geq x \geq 3$
R10M5	$y_{25} = 1.1968 \times x^{-0.323}$	0.9455	$365 \geq x \geq 3$
R10M7.5	$y_{25} = 1.1295 \times x^{-0.357}$	0.9577	$365 \geq x \geq 3$

For each concrete mix, one linear equation between the percentage of chloride ions at 25-35 mm depth ('y_{25}') and at 10-20 mm depth ('y_{10}') was developed by regression analysis with a high coefficient of determination (R^2) as shown in Table 7.27.

Table 7.27 Mathematical relation between chloride percentage at 25-35 mm depth ('y_{25}') and at 10-20 mm depth ('y_{10}')

Mix	Prediction Models	R^2	Validity
R0	$y_{25} = 0.9779 \times y_{10} - 0.0132$	0.9998	$y_{10} > 0.0135$
R10	$y_{25} = 1.0045 \times y_{10} - 0.0216$	0.9972	$y_{10} > 0.022$
M2.5	$y_{25} = 1.032 \times y_{10} - 0.0815$	0.9941	$y_{10} > 0.079$
M5	$y_{25} = 0.9887 \times y_{10} - 0.0057$	0.9985	$y_{10} > 0.006$
M7.5	$y_{25} = 0.9043 \times y_{10} + 0.0403$	0.9933	$y_{10} > 0$
M10	$y_{25} = 0.9907 \times y_{10} - 0.0142$	0.9991	$y_{10} > 0.015$
R5M5	$y_{25} = 0.9338 \times y_{10} + 0.0141$	0.9995	$y_{10} > 0$
R5M7.5	$y_{25} = 1.0259 \times y_{10} - 0.0519$	0.9723	$y_{10} > 0.051$
R10M5	$y_{25} = 0.9246 \times y_{10} + 0.0128$	0.9842	$y_{10} > 0$
R10M7.5	$y_{25} = 0.9 \times y_{10} - 2 \times 10^{-16}$	0.9999	$y_{10} > 2.23\times10^{-16}$

One linear equation (valid for all concrete mix at all curing age) between the percentage of chloride ions at 25-35 mm depth ('y_{25}') and at 10-20 mm depth ('y_{10}') was developed as shown in Equation 7.12 (R^2 = 0.9928).

$$y_{25} = 0.976 \times y_{10} - 0.0137 \qquad (y_{10} > 0.015) \qquad 7.12$$

7.9.5 Relationship between Water Absorption and Chloride Ion Penetration

The regression equations were generated using the experimental findings (equations given in Table 7.20, Table 7.21, Table 7.22, Table 7.24, Table 7.25 and Table 7.26). It was done to predict one parameter from another without the need to perform an experiment on concrete admixed with RSA and MS. These equations were then used to predict saturated water absorption, rate of water absorption, coefficient of water absorption and chloride ion penetration from curing age. Subsequently, predictive graphs (Figure 7.21) were plotted between the predicted parameters and curing age. The predictive graphs can be helpful in making arrangements about conceivable outcomes.

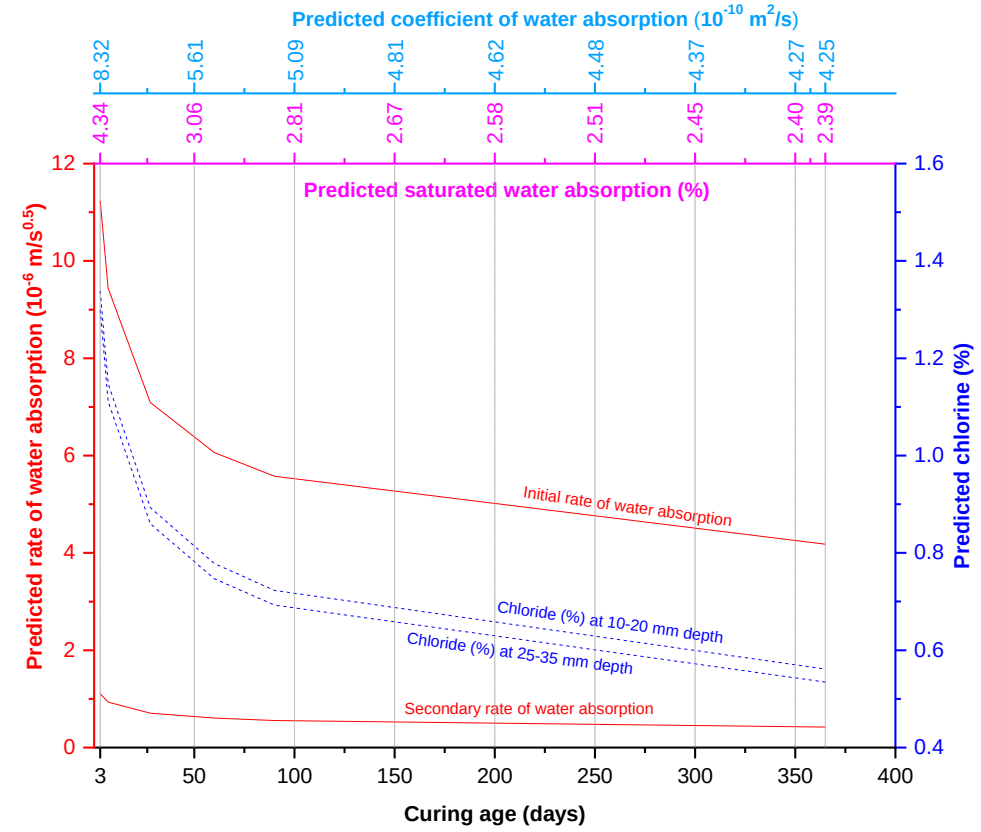
Predicted coefficient of water absorption (10^-10 m^2/s)
8.32
5.61
5.09
4.81
4.62
4.48
4.37
4.27
4.25
4.34
3.06
2.81
2.67
2.58
2.51
2.45
2.40
2.39
Predicted saturated water absorption (%)
Predicted rate of water absorption (10^-6 m/s^0.5)
Predicted chlorine (%)
Initial rate of water absorption
Chloride (%) at 10-20 mm depth
Chloride (%) at 25-35 mm depth
Secondary rate of water absorption
Curing age (days)

a) R0

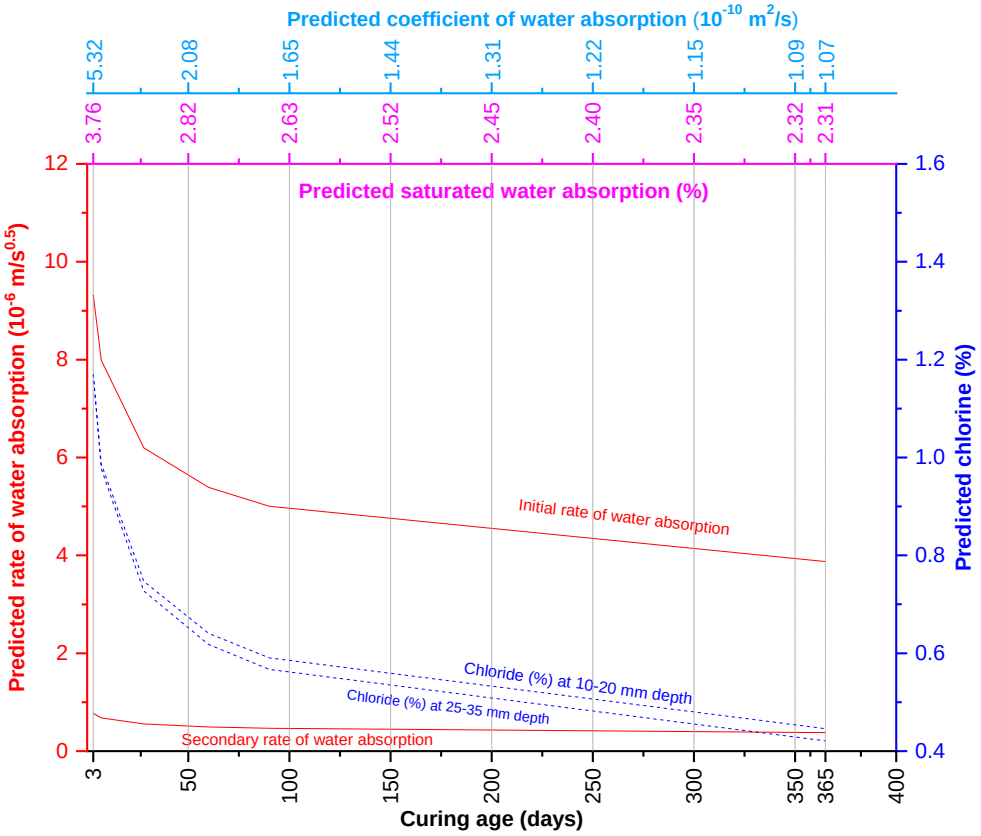
Predicted coefficient of water absorption (10^-10 m^2/s)
5.32
2.08
1.65
1.44
1.31
1.22
1.15
1.09
1.07
3.76
2.82
2.63
2.52
2.45
2.40
2.35
2.32
2.31
Predicted saturated water absorption (%)
Predicted rate of water absorption (10^-6 m/s^0.5)
Predicted chlorine (%)
Initial rate of water absorption
Chloride (%) at 10-20 mm depth
Chloride (%) at 25-35 mm depth
Secondary rate of water absorption
Curing age (days)

b) R10

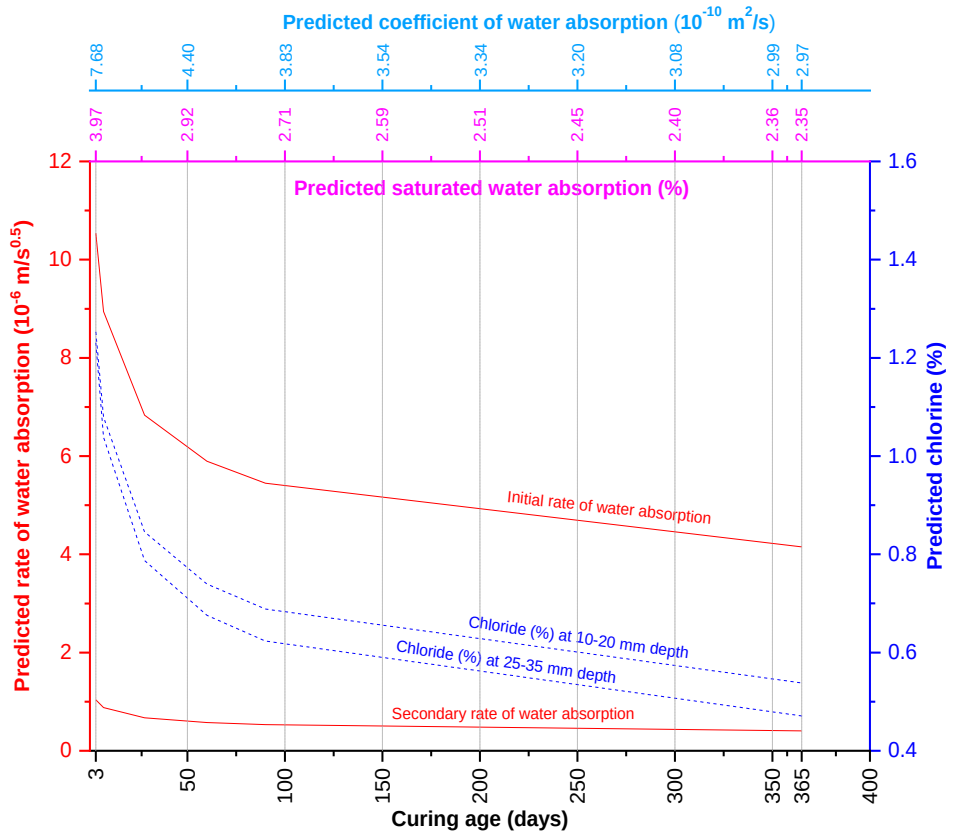
Predicted coefficient of water absorption (10^-10 m^2/s)
7.68
4.40
3.83
3.54
3.34
3.20
3.08
2.99
2.97
3.97
2.92
2.71
2.59
2.51
2.45
2.40
2.36
2.35
Predicted saturated water absorption (%)
Predicted rate of water absorption (10^-6 m/s^0.5)
Predicted chlorine (%)
Initial rate of water absorption
Chloride (%) at 10-20 mm depth
Chloride (%) at 25-35 mm depth
Secondary rate of water absorption
Curing age (days)

c) M2.5

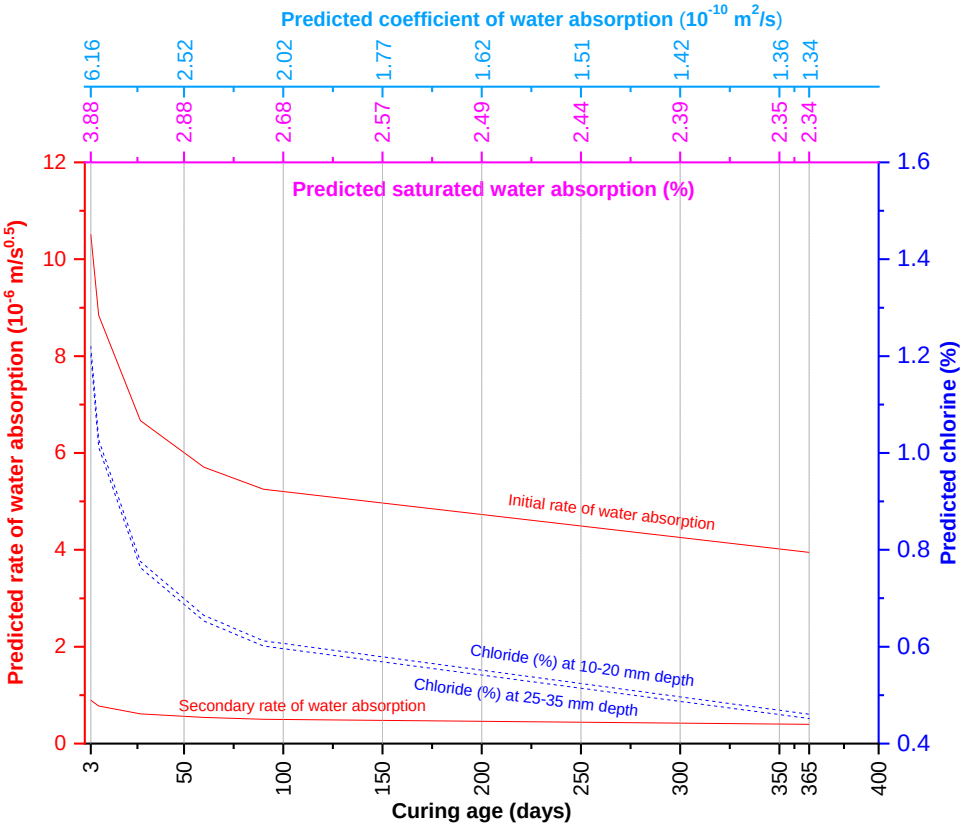
Predicted coefficient of water absorption (10^-10 m^2/s)
6.16
2.52
2.02
1.77
1.62
1.51
1.42
1.36
1.34
3.88
2.88
2.68
2.57
2.49
2.44
2.39
2.35
2.34
Predicted saturated water absorption (%)
Predicted rate of water absorption (10^-6 m/s^0.5)
Predicted chlorine (%)
Initial rate of water absorption
Chloride (%) at 10-20 mm depth
Chloride (%) at 25-35 mm depth
Secondary rate of water absorption
Curing age (days)

d) M5

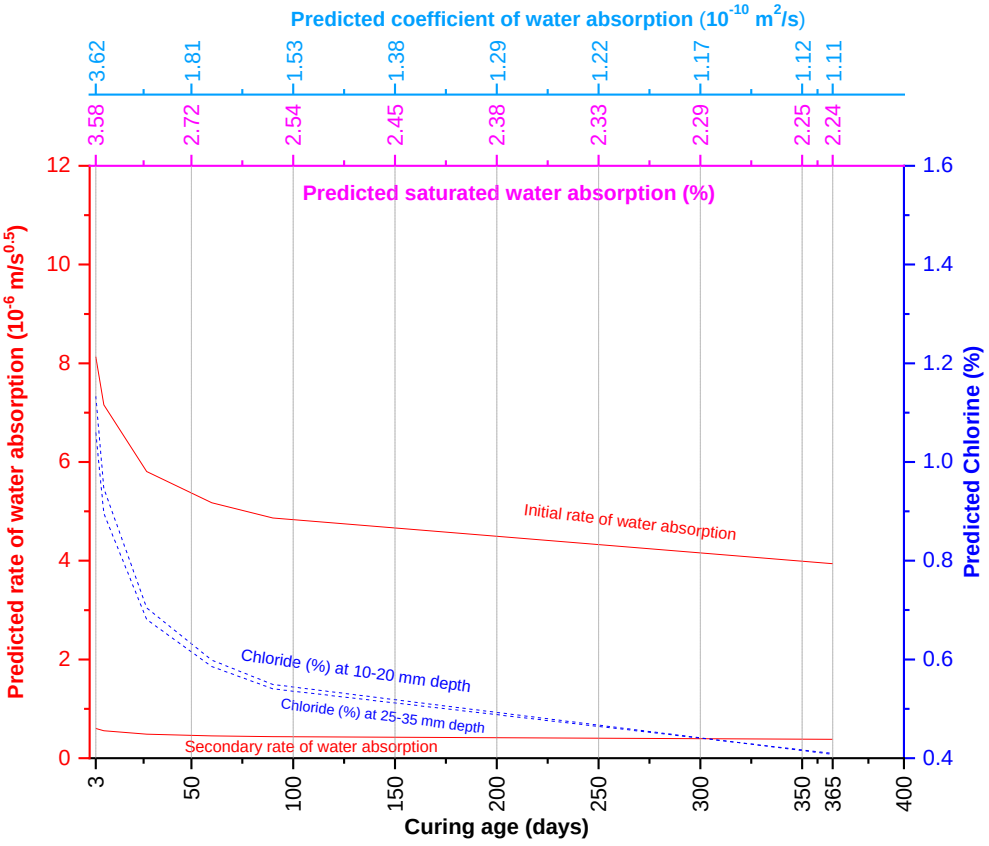
Predicted coefficient of water absorption (10^-10 m^2/s)
3.62
1.81
1.53
1.38
1.29
1.22
1.17
1.12
1.11
3.58
2.72
2.54
2.45
2.38
2.33
2.29
2.25
2.24
Predicted saturated water absorption (%)
Predicted rate of water absorption (10^-6 m/s^0.5)
Predicted Chlorine (%)
Initial rate of water absorption
Chloride (%) at 10-20 mm depth
Chloride (%) at 25-35 mm depth
Secondary rate of water absorption
Curing age (days)

e) M7.5

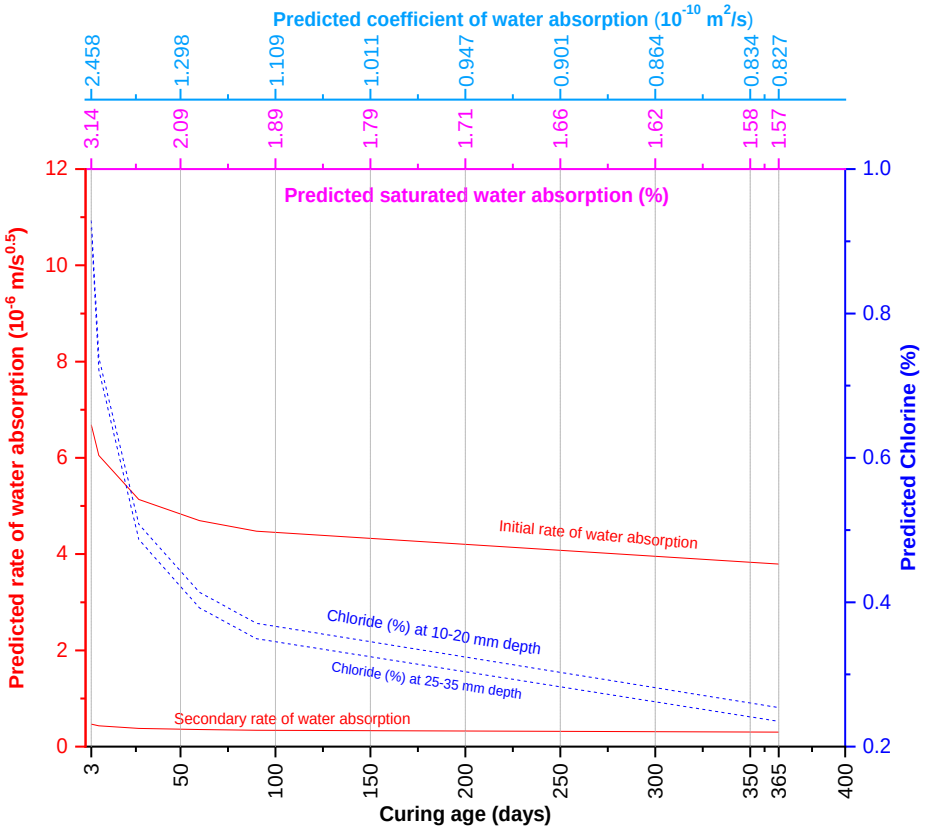
Predicted coefficient of water absorption (10^-10 m^2/s)
2.458
1.298
1.109
1.011
0.947
0.901
0.864
0.834
0.827
3.14
2.09
1.89
1.79
1.71
1.66
1.62
1.58
1.57
Predicted saturated water absorption (%)
Predicted rate of water absorption (10^-6 m/s^0.5)
Predicted Chlorine (%)
Initial rate of water absorption
Chloride (%) at 10-20 mm depth
Chloride (%) at 25-35 mm depth
Secondary rate of water absorption
Curing age (days)

f) M10

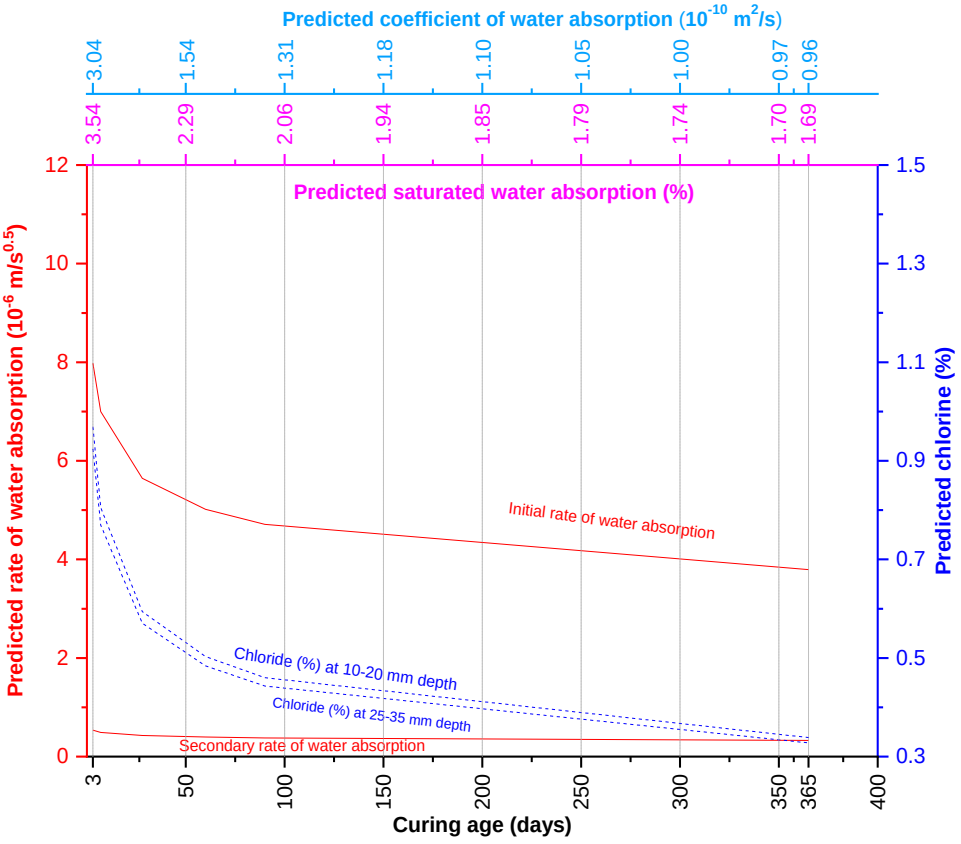

g) R5M5

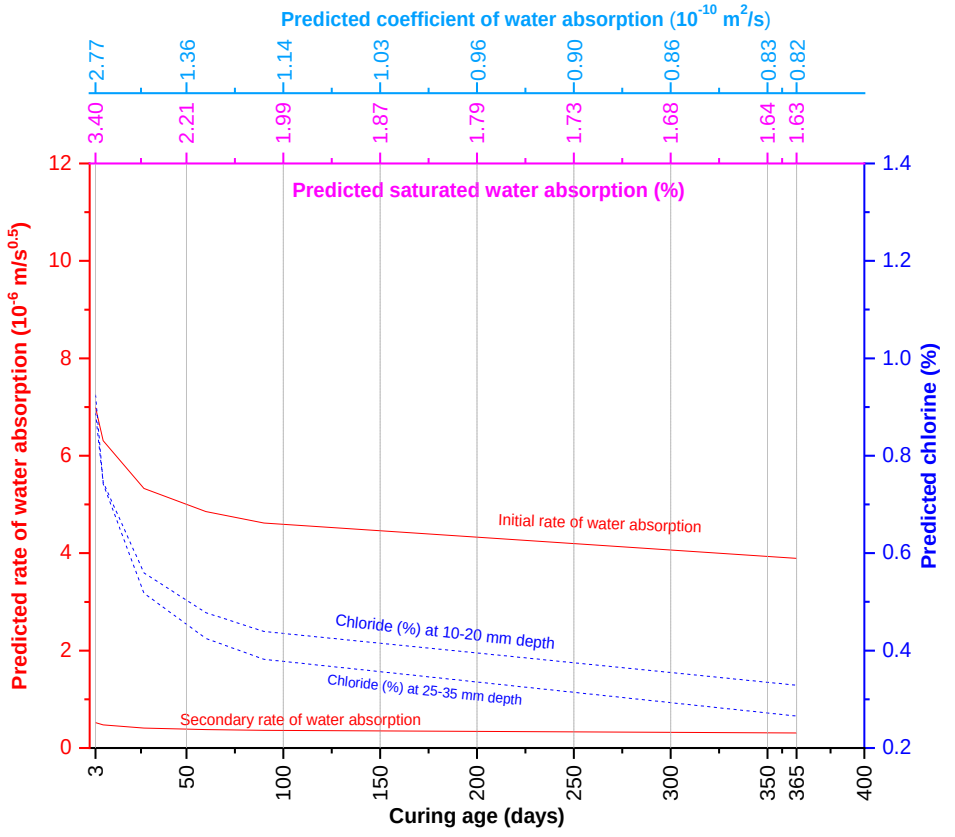

h) R5M7.5

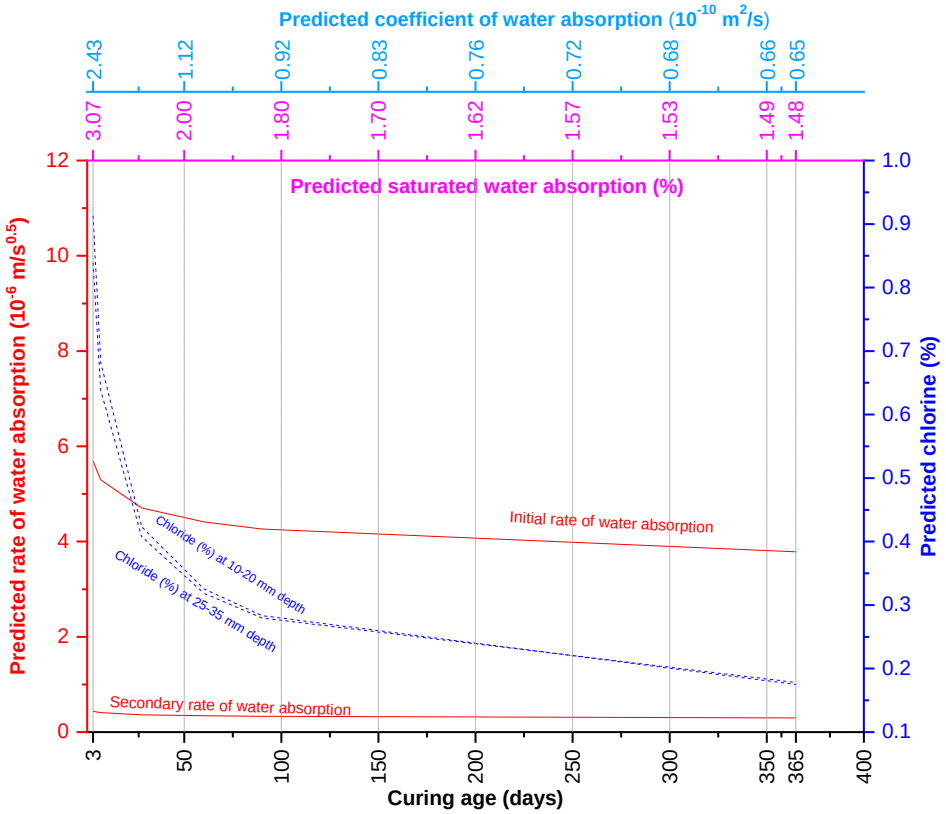

i) R10M5

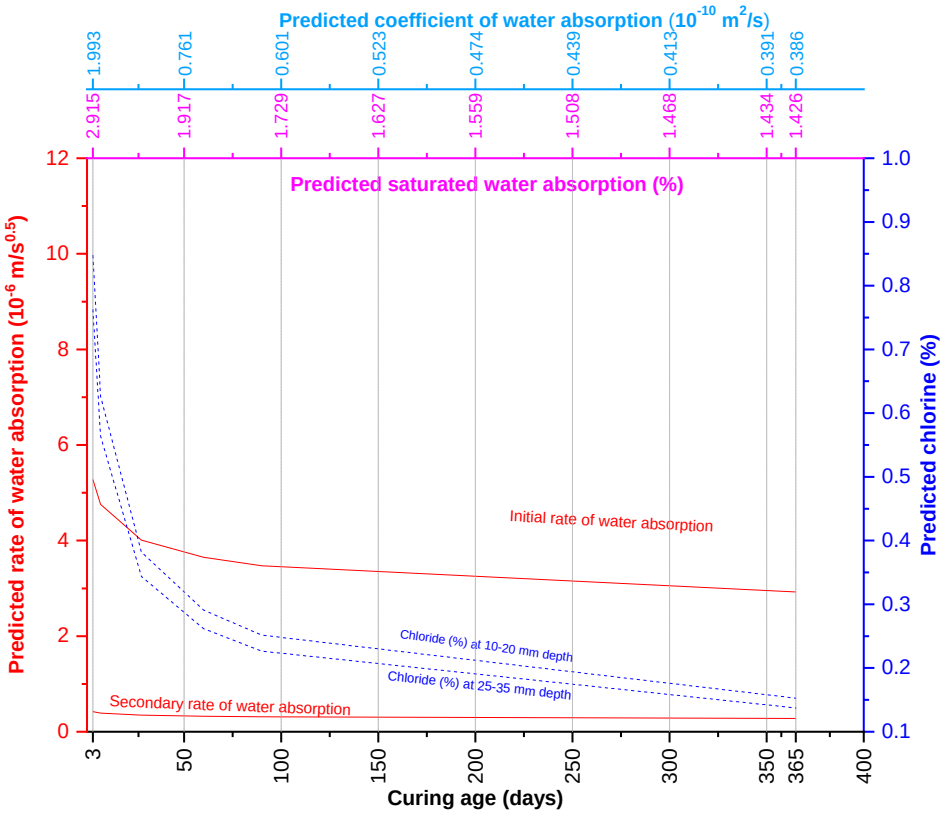

j) R10M7.5

Figure 7.21 Predictive charts of the various mix for M40 grade PQC **(a)** R0 (**b)** R10 (**c)** M2.5 (**d)** M5 (**e)** M7.5 (**f)** M10 (**g)** R5M5 (**h)** R5M7.5 (**i)** R10M5 (**j)** R10M7.5

7.9.6 Acidic Environment

The percentage mass loss in concrete ('l_m') after 30 days immersion in acidic solution was found to be dependent on the percentage of rice straw ash ('r'), percentage of microsilica ('m') and curing days in water ('x'). Mathematical models for percentage loss of mass in concrete having w/c ratio of 0.39 were developed using the experimental values and are presented in Table 7.28. These equations were derived from the experimental data given in Table 7.14.

Table 7.28 Mathematical models for percentage mass loss ('l_m')

Type of Acidic Solution	Prediction Models	R^2
Hydrochloric Acid	$4.086 - 0.072 \times r - 0.134 \times m - 0.004 \times x$	0.9394
Sulphuric Acid	$3.312 - 0.048 \times r - 0.095 \times m - 0.003 \times x$	0.9730

The percentage loss of compressive strength in concrete ('l_c') due to 30 days immersion in acidic solution was found to be dependent on the percentage of rice straw ash ('r'), percentage of microsilica ('m') and days of water curing ('x'). Mathematical models for percentage loss of compressive strength having w/b ratio of 0.39 were developed using the experimental values and are presented in Table 7.29. These equations were derived from the experimental data given in Table 7.17.

Table 7.29 Mathematical models for percentage loss of compressive strength ('l_c')

Type of Acidic Solution	Prediction Models	R^2
Hydrochloric Acid	$8.020 - 0.209 \times r - 0.408 \times m - 0.006 \times x$	0.9590
Sulphuric Acid	$6.015 - 0.174 \times r - 0.352 \times m - 0.005 \times x$	0.8636

The percentage loss of compressive strength in concrete ('l_c') due to 30 days immersion in acidic solution was also found to be dependent on the respective percentage loss of mass ('l_m'), and the equations between them in two different acidic solutions are given in Table 7.30. It was observed that the percentage loss of mass would be equal to the percentage loss of compressive strength at 15% for HCl solution

and 2.41% for H_2SO_4 solution at 28 days of water curing, and at 1.25% for HCl solution and 0.17% for H_2SO_4 solution at 365 days of water curing.

Table 7.30 Mathematical models between percentage loss of compressive strength ('l_c') and percentage mass loss ('l_m')

Type of Acidic Solution	Water Curing Age	Prediction Models	R^2	Validity
Hydrochloric Acid	28 days	$l_c = 2 + 0.8667 \times l_m$	0.965	l_m >0
	365 days	$l_c = -2.5 + 3.006 \times l_m$	0.939	l_m >0.84
Sulphuric Acid	28 days	$l_c = -3.27 + 2.35 \times l_m$	0.938	l_m >1.39
	365 days	$l_c = -0.034 + 1.2 \times l_m$	0.975	l_m >0.03

The compressive strength of concrete ('f_{ca}') at 28 days and 365 days of water curing and subsequent acid immersion was found to be dependent on the compressive strength of respective concrete at 58 and 395 days of water curing ('f_c') respectively and the equations between them are given in Table 7.31.

Table 7.31 Mathematical models between compressive strength under water curing and acidic immersion ('f_{ca}') and compressive strength under water curing ('f_c')

Type of Acidic Solution	Water Curing Age	Prediction Models	R^2	Validity
Hydrochloric acid	28 days	$f_{ca} = -7.72 + 1.1 \times f_c$	0.999	f_c >7.02
	365 days	$f_{ca} = -8.69 + 1.128 \times f_c$	0.998	f_c >7.71
Sulphuric acid	28 days	$f_{ca} = -6.77 + 1.098 \times f_c$	0.999	f_c >6.17
	365 days	$f_{ca} = -3.61 + 1.047 \times f_c$	0.999	f_c >3.45

7.9.7 Accelerated Carbonation Curing

The compressive (f_c'), flexural (f_r') and split tensile (f_t') strength of concrete at 28 days of combined curing (14 days water + 14 days ACC) were found to be dependent on the respective compressive (f_c), flexural (f_r) and split tensile (f_t) strength of concrete at 28 days of curing in water. Mathematical models for various strength of concrete after combined curing at w/c ratio of 0.39 were developed using the experimental values and are presented in Table 7.32. These equations were derived from the experimental data given in Table 7.18.

Table 7.32 Mathematical models for strength after 14 days water+14 days ACC

Strength Type	Prediction Model	R^2	Validity
compressive (f_c')	$0.6871 \times f_c + 17.2$	0.9530	$f_c \geq 0$
flexural (f_r')	$0.8306 \times f_r + 1.0838$	0.9813	$f_r \geq 0$
split tensile (f_t')	$1.0911 \times f_t - 0.3279$	0.9928	$f_t \geq 0.4$

The depth of carbonation in concrete ('d') subjected to 28 days of combined curing (ACC + water) was found to be dependent on the respective compressive strength ('f_c') of concrete subjected to 28 days of water curing as given in Equation 7.13 (R^2 = 0.9529).

$$d = 5 \times 10^{13} \times 2.718^{(-0.568) \times f_c} \quad 7.13$$

7.10 CONCLUSIONS

The experiments performed in this chapter to analyse the mechanical strength of cement concrete admixed with RSA and MS led to the following conclusions:

- When OPC was replaced by a composite of RSA and MS by more than or equal to 15%, the air content of the fresh concrete became constant.

- The admixing of MS and RSA causes a reduction in the saturated water absorption of admixed concrete. The lowest value of saturated water absorption was obtained in concrete of mix R10M7.5 (10% RSA-7.5% MS). MS was more effective than RSA in reducing the water absorption capacity of concrete.

- Rice straw ash and microsilica were much more effective in reducing the secondary rate of water absorption as compared to the initial rate of water absorption of concrete. The initial rate of water absorption of each concrete mix was mostly constant when concrete was subjected to more than 28 days of curing in water. The

lowest rate of water absorption in concrete was observed in the concrete of mix R10M7.5. A linear equation between initial ('y_i') and secondary ('y_s') rate of water absorption was developed which was valid for all concrete mix at all curing age ($y_s = 0.0892 \times y_i - 0.02$).

- Due to the admixing of RSA and MS and also due to an increase in the curing age, the defence mechanism of concrete to chloride ions penetration improves significantly. At 10-20 mm and 25-35 mm depth, the chloride penetration in every concrete mix was constant when concrete was subjected to curing in water for more than 28 days. A common linear equation between chloride percentage at 10-20 mm depth ('y_{10}') and 25-35 mm depth ('y_{25}') was developed which was valid for each concrete mix at any curing age ($y_{25} = 0.976 \times y_{10} - 0.0137$).

- The improvement in the resistance of concrete to acid attack was higher when it was admixed with microsilica as compared to when it was admixed with RSA.

- HCl solution was more corrosive to concrete admixed with RSA and MS as compared to H_2SO_4 solution.

- The difference between the percentage loss of mass in concrete due to attack of HCl and H_2SO_4 decreases with an increase in the proportion of mineral admixtures. Curing of concrete for longer duration hardened it to the extent that acid penetration was same irrespective of the type of acid solution.

- In XRD analysis of concrete samples subjected to acidic immersion, the intensities of $CaCl_2$ under HCl solution and gypsum and ettringite under H_2SO_4 solution were lowest in the concrete of mix R10M7.5.

- When percentage increase in concrete strength due to combined curing was calculated with respect to the respective strength due to water curing, rice straw ash was more effective in case of compressive and flexural strength while microsilica was more effective in case of split tensile strength.

- The depth of carbonation in concrete admixed with RSA was more than the carbonation depth in concrete admixed with MS and lesser than the control concrete.

- The carbonation depth in concrete at 28 days of combined curing decreases with an increase in its compressive strength.